

Reactive Extraction of Metal Ion and Simultaneous Stripping Using Nanofibers-
Supported Liquid Membrane in a Microchannel



A Thesis Submitted in Partial Fulfillment of the Requirements
for the Degree of Master of Engineering in Chemical Engineering

Department of Chemical Engineering

Faculty of Engineering

Chulalongkorn University

Academic Year 2018

Copyright of Chulalongkorn University

การสกัดแบบมีปฏิกิริยาของไอออนโลหะและการนำกลับพร้อมกันโดยใช้เยื่อแผ่นเหลวที่พองอยู่บน
เส้นใยนาโนในช่องการไหลระดับไมโคร



วิทยานิพนธ์นี้เป็นส่วนหนึ่งของการศึกษาตามหลักสูตรปริญญาวิศวกรรมศาสตรมหาบัณฑิต
สาขาวิชาวิศวกรรมเคมี ภาควิชาวิศวกรรมเคมี
คณะวิศวกรรมศาสตร์ จุฬาลงกรณ์มหาวิทยาลัย
ปีการศึกษา 2561
ลิขสิทธิ์ของจุฬาลงกรณ์มหาวิทยาลัย

Thesis Title	Reactive Extraction of Metal Ion and Simultaneous Stripping Using Nanofibers-Supported Liquid Membrane in a Microchannel
By	Miss Nattakarn Chucherd
Field of Study	Chemical Engineering
Thesis Advisor	Associate Professor VARONG PAVARAJARN, Ph.D.

Accepted by the Faculty of Engineering, Chulalongkorn University in Partial Fulfillment of the Requirement for the Master of Engineering

..... Dean of the Faculty of Engineering
(Professor SUPOT TEACHAVORASINSKUN, D.Eng.)

THESIS COMMITTEE

..... Chairman
(Professor MUENDUEN PHISALAPHONG, Ph.D.)

..... Thesis Advisor
(Associate Professor VARONG PAVARAJARN, Ph.D.)

..... Examiner
(Pongtorn Charoensuppanimit, Ph.D.)

..... External Examiner
(Chanchana Thanachayanont)

ณัฐกานต์ ชูเชิด : การสกัดแบบมีปฏิกิริยาของไอออนโลหะและการนำกลับพร้อมกันโดย
ใช้เยื่อแผ่นเหลวที่พองอยู่บนเส้นใยนาโนในช่องการไหลระดับไมโคร. (Reactive
Extraction of Metal Ion and Simultaneous Stripping Using Nanofibers-
Supported Liquid Membrane in a Microchannel) อ.ที่ปรึกษาหลัก : รศ. ดร.วรงค์
ปวรอาจารย์

โลหะหนักในน้ำเสียที่เกิดจากภาคอุตสาหกรรมเป็นเรื่องที่ต้องตระหนักถึงความสำคัญ
สำหรับปัญหาทางด้านสิ่งแวดล้อมและเศรษฐกิจ งานวิจัยฉบับนี้จึงมีจุดมุ่งหมายที่จะนำกลับไอออน
ของโลหะหนักจากน้ำเสีย โดยใช้การสกัดแบบมีปฏิกิริยาโดยเยื่อแผ่นเหลวที่พองอยู่บนเส้นใยนาโน
ในช่องการไหลระดับไมโคร ซึ่งกระบวนการนี้สามารถเกิดปฏิกิริยาการสกัดและการนำกลับไอออน
ของโลหะหนักได้ในเวลาเดียวกัน นอกจากนี้การประยุกต์ใช้ช่องการไหลระดับไมโครสามารถลด
ความต้านทานการแพร่ของมวลสาร ส่งผลให้ประสิทธิภาพโดยรวมของการสกัดดีขึ้น ไอออนของ
โลหะทองแดงถูกนำมาใช้เป็นตัวแทนของโลหะหนักในน้ำเสียและได-(2-เอทิลเฮกซิล) ฟอสฟอริกแ
ซิด ละลายในโครซีนถูกใช้เป็นตัวแทนของสารสกัด โดยสารสกัดจะถูกตรึงไว้บนเส้นใยนาโนพอลิไวนิลลิดีน
ฟลูออไรด์ การทดลองได้ดำเนินการขึ้นโดยมีวัตถุประสงค์เพื่อระบุขึ้นกำหนดอัตราสำหรับ
กระบวนการสกัดนี้ จากผลการทดลองพบว่าการแพร่ไอออนของทองแดงจากสารละลายไปยัง
บริเวณผิวของเยื่อแผ่นเหลวและการแพร่ของสารเชิงซ้อนของโลหะทองแดงข้ามผ่านเยื่อแผ่นเหลว
ไม่ได้เป็นขึ้นกำหนดอัตรา ในการคำนวณหาอัตราการเกิดปฏิกิริยาพบว่าอัตราการเกิดปฏิกิริยาของ
กระบวนการสกัดมีค่าสูงกว่าอัตราการเกิดปฏิกิริยาของกระบวนการนำกลับ จึงสรุปได้ว่าขั้นตอน
กระบวนการนำกลับไอออนของโลหะคอปเปอร์เป็นขึ้นกำหนดอัตรา นอกจากนี้ความสามารถใน
การสกัดไอออนของโลหะขึ้นอยู่กับปัจจัยต่าง ๆ ได้แก่ ความเข้มข้นเริ่มต้นของไอออน ความหนา
ของช่องการไหลระดับไมโครและอัตราการป้อนของสารละลาย จากผลการทดลองพบว่าสามารถ
สกัดไอออนของโลหะทองแดงได้ประสิทธิภาพสูงถึง 82% ที่ความเข้มข้นเริ่มต้นของโลหะไอออน 1
กรัมต่อลิตร ที่ความหนาช่องการไหล 125 ไมโครเมตร และอัตราการไหลที่ 9 มิลลิลิตรต่อชั่วโมง

สาขาวิชา วิศวกรรมเคมี
ปีการศึกษา 2561

ลายมือชื่อนิสิต
ลายมือชื่อ อ.ที่ปรึกษาหลัก

6070177621 : MAJOR CHEMICAL ENGINEERING

KEYWORD: Reactive extraction, Supported liquid membranes, Microchannel,
Nanofibers

Nattakarn Chucherd : Reactive Extraction of Metal Ion and Simultaneous Stripping Using Nanofibers-Supported Liquid Membrane in a Microchannel.
Advisor: Assoc. Prof. VARONG PAVARAJARN, Ph.D.

Heavy metals in wastewater resulting from industries have become a prime concern for both environmental and economic reasons. This work intends to recover ions of heavy metal from wastewater using reactive extraction by nanofibers-supported liquid membrane (NSLM) in a microchannel. The use of supported liquid membrane enables simultaneous extraction and stripping (*i.e.*, recovery of the extractant) processes. In this study, the NSLM was applied in a microchannel to minimize mass transfer resistance, hence improving overall performance of the extraction. Copper (II) ion was used as a model ion, while di-2-ethylhexyl phosphoric acid (D2EHPA) dissolved in kerosene was used as the extractant. The extractant was supported by a thin layer of polyvinylidene fluoride (PVDF) nanofibers to form a thin immiscible layer. The experiment was conducted to identify the rate determining step in this process. The results show that the reactive stripping step was the rate determining step. The efficiency of extraction Cu(II) ions can be as high as 82% at 1 g/L of initial concentration of Cu(II) ion, microchannel thickness of 125 μm and flow rate of 9 ml/h.

Field of Study: Chemical Engineering

Student's Signature

Academic Year: 2018

Advisor's Signature

ACKNOWLEDGEMENTS

Firstly, I would like to express my gratitude to my advisor, Associate Professor Varong Pavarajarn, for their advice. I get experience in practical problem-solving skills. I think that these skills are also very valuable for developing my attitude.

Furthermore, I would also like to thank to Professor Muenduen Phisalpong as a chairman, Dr. Pongtorn Charoensuppanimit and Dr. Chanchana Thanachayanont, as a member of the thesis committee, for their recommendations.

Most of all, I would like to extend my thanks to the member of the Center of Excellence in Particle Technology, Department of Chemical Engineering, Faculty of Engineering, Chulalongkorn University. Especially, people at the 11th floor, for their suggestions and encouragements.

Finally, I would like to thank my parents for their support and continuous encouragement throughout my years of study and through the process of researching and writing this thesis.



จุฬาลงกรณ์มหาวิทยาลัย
CHULALONGKORN UNIVERSITY

Nattakarn Chucherd

TABLE OF CONTENTS

	Page
ABSTRACT (THAI).....	iv
ABSTRACT (ENGLISH).....	v
ACKNOWLEDGEMENTS.....	vi
TABLE OF CONTENTS.....	vii
LIST OF TABLE.....	x
LIST OF FIGURE.....	xi
CHAPTER I Introduction.....	1
CHAPTER II THEORY AND LITERATURE REVIEWS.....	4
2.1 Liquid membrane (LM).....	4
2.1.1 Bulk liquid membrane (BLM).....	4
2.1.2 Emulsion liquid membranes (ELM).....	5
2.1.3 Supported liquid membranes (SLM).....	5
2.1.4 The components used in Liquid Membrane.....	7
2.1.5 The transport of heavy metal ions through liquid membrane.....	11
2.1.6 The advantages and disadvantages of support liquid membrane.....	12
2.1.7 The effect of various parameters on the liquid membrane (LM) extraction process.....	14
2.2 Poly (vinylidene fluoride) (PVDF).....	17
2.3 Electrospinning process.....	19
2.4 Microreactor.....	21
CHAPTER III EXPERIMENTALS.....	22

3.1 Reagent	22
3.2 Apparatus.....	22
3.2.1 Acrylic plates	23
3.2.2 Teflon sheets.....	23
3.2.3 Collector Sieve plate	24
3.3 Fabrication of PVDF nanofibers membrane.....	24
3.4 Experimental procedures	25
3.5 Analysis.....	25
CHAPTER IV RESULTS AND DISCUSSION.....	28
4.1 The surface morphology of PVDF nanofibers membrane	28
4.2 The reactive extraction of metal ion.....	30
4.2.1 Effect of microchannel thickness on reactive extraction	31
4.2.2 Effect of flow rate on reactive extraction.....	34
4.3 The reactive stripping of metal ion.....	37
4.3.1 Effect of microchannel thickness on reactive stripping	38
4.3.2 Effect of flow rate on reactive stripping.....	41
4.4 Simultaneous reactive extraction and stripping of metal ion	44
4.4.1 Effect of membrane thickness	45
4.4.2 Effect of initial Cu(II) concentration in the feed phase	47
4.4.3 Effect of microchannel thickness.....	50
4.4.4 Effect of flow rate	52
CHAPTER V CONCLUSIONS AND RECOMMENDATIONS.....	54
5.1 Conclusions	54
5.2 Recommendation	54

APPENDIX.....	55
APPENDIX A Calibration Data Analysis.....	56
APPENDIX B PROCEDURE OF CHEMICAL PREPARATION	58
APPENDIX C CALCULATION.....	59
APPENDIX D RAW DATA.....	61
REFERENCES.....	74
VITA.....	78



LIST OF TABLE

	Page
Table 1 Literature review of material support for SLM process	9
Table 2 Compositions and conditions of LM on copper removal	10
Table 3 The physical properties of PVDF	18
Table 4 Electrospinning parameters and their effects on fiber morphology	20
Table 5 The outlet concentration of Cu(II) ion at different microchannel thickness on the reactive extraction	33
Table 6 The outlet concentration of Cu(II) ion at steady state with different flow rate	35
Table 7 The outlet concentration of Cu(II) ion at different microchannel thickness on the reactive stripping	39
Table 8 The outlet concentration of Cu(II) ion at steady state with different flow rate	42
Table 9 The outlet concentration of Cu(II) ion with different thickness of membrane on reactive extraction and stripping	46
Table 10 The outlet concentration of Cu(II) ion with different initial concentration on reactive extraction and stripping	49
Table 11 The outlet concentration of Cu(II) ion with different microchannel thickness on reactive extraction and stripping	51
Table 12 The outlet concentration of Cu(II) ion with different flow rate on reactive extraction and stripping	53

LIST OF FIGURE

	Page
Figure 1 Facilitated transport of Cu^{2+} through liquid membranes using a carrier mediated co-transport mechanism.	6
Figure 2 Schematic diagram of flat sheet supported liquid membrane (FSSLM) in membrane separation process	7
Figure 3 Hollow fiber supported liquid membranes (HFSLM).....	7
Figure 4 Transport mechanism of the Cu(II) ions	11
Figure 5 Copper (II) complex structure.....	12
Figure 6 Effect of D2EHPA concentration in membrane phase of Cu(II) flux. (Experimental conditions: feed phase: 15.7×10^{-4} mol/L; strip phase: 1 M H_2SO_4).....	15
Figure 7 Effect of initial Cu(II) concentration on the transport flux. (Experimental conditions: strip phase: 1 M H_2SO_4 ; D2EHPA concentration in PIM: 4.8×10^{-2} mol/L.)... ..	16
Figure 8 Electrospinning schematic formation by electrospinning.....	20
Figure 9 Diagram showing fiber	20
Figure 10 The components of microreactor	22
Figure 11 Acrylic plates	23
Figure 12 Teflon sheets	23
Figure 13 Collector Sieve plate	24
Figure 14 The experimental set up of PVDF nanofibers membrane synthesis by electrospinning method.....	25
Figure 15 UV-Visible spectrophotometer.....	26
Figure 16 The photograph of TOC analyzer.....	27
Figure 17 (a) FE-SEM images of electrospinning PVDF nanofibers membranes (b) The nanofiber diameter histograms.....	29

Figure 18 Effect of microchannel thickness on the rate of reactive extraction	33
Figure 19 Effect of microchannel thickness on the %extraction of Cu(II) ion.....	34
Figure 20 Effect of residence time on the %extraction of Cu(II) ion.....	35
Figure 21 Pseudo-second order kinetic model of reactive extraction of Cu(II) ion	36
Figure 22 Effect of residence time on the rate of reactive extraction	37
Figure 23 Effect of microchannel thickness on the rate of reactive stripping	40
Figure 24 Effect of microchannel thickness on the %stripping of Cu(II) ion.....	40
Figure 25 Effect of residence time on the %stripping of Cu-D2EHPA complex.....	42
Figure 26 Pseudo-second order kinetic model of reactive stripping of Cu(II) ions	43
Figure 27 Effect of residence time on the rate of reactive stripping	44
Figure 28 Effect of membrane thickness on simultaneous reactive extraction and stripping	46
Figure 29 Concentration of CuSO ₄ at any time in feed phase.....	49
Figure 30 Effect of initial concentration of Cu(II) ion in the feed phase on simultaneous reactive extraction and stripping	50
Figure 31 Effect of microchannel thickness on the simultaneous reactive extraction and stripping of Cu(II) ions	51
Figure 32 Effect of residence time on the simultaneous reactive extraction and stripping of Cu(II) ions	53
Figure 33 Calibration curve of Cu(II) ion in the range of 5-25 g/L	56
Figure 34 Calibration curve of Cu(II) ion in the range of 0.2-1.2 g/L	56
Figure 35 Calibration curve of Cu(II) ion in HCl Solution	57
Figure 36 Calibration curve of Cu-D2EHPA complex concentration	57
Figure 37 The concentration of Cu(II) ion in the feed phase and membrane phase at any time (thickness = 175 μm).....	61

Figure 38 The concentration of Cu(II) ion in the feed phase and stripping phase at any time (thickness = 300 μm).....	61
Figure 39 The concentration of Cu(II) ion in the feed phase and stripping phase at any time (thickness = 425 μm).....	62
Figure 40 The concentration of Cu(II) ion in the feed phase and membrane phase at any time (Flow rate = 12 ml/h).....	62
Figure 41 The concentration of Cu(II) ion in the feed phase and membrane phase at any time (Flow rate = 18 ml/h).....	63
Figure 42 The concentration of Cu(II) ion in the feed phase and membrane phase at any time (Flow rate = 27 ml/h).....	63
Figure 43 The concentration of Cu(II) ion in the membrane phase and stripping phase at any time (thickness = 175 μm).....	64
Figure 44 The concentration of Cu(II) ion in the membrane phase and stripping phase at any time (thickness = 300 μm).....	64
Figure 45 The concentration of Cu(II) ion in the membrane phase and stripping phase at any time (thickness = 425 μm).....	65
Figure 46 The concentration of Cu(II) ion in the membrane phase and stripping phase at any time (Flow rate = 12 ml/h).....	65
Figure 47 The concentration of Cu(II) ion in the membrane phase and stripping phase at any time (Flow rate = 18 ml/h).....	66
Figure 48 The concentration of Cu(II) ion in the membrane phase and stripping phase at any time (Flow rate = 27 ml/h).....	66
Figure 49 The concentration of Cu(II) ion in the feed phase and stripping phase at any time (initial concentration = 10 g/L).....	67
Figure 50 The concentration of Cu(II) ion in the feed phase and stripping phase at any time (initial concentration = 5 g/L).....	67

Figure 51 The concentration of Cu(II) ion in the feed phase and stripping phase at any time (initial concentration = 1 g/L)	68
Figure 52 The concentration of Cu(II) ion in the feed phase and stripping phase at any time (initial concentration = 0.5 g/L).....	68
Figure 53 The concentration of Cu(II) ion in the feed phase and stripping phase at any time (thickness = 125 μm).....	69
Figure 54 The concentration of Cu(II) ion in the feed phase and stripping phase at any time (thickness = 250 μm).....	69
Figure 55 The concentration of Cu(II) ion in the feed phase and stripping phase at any time (thickness = 500 μm).....	70
Figure 56 The concentration of Cu(II) ion in the feed phase and stripping phase at any time (Flow rate = 12 ml/h).....	70
Figure 57 The concentration of Cu(II) ion in the feed phase and stripping phase at any time (Flow rate = 18 ml/h).....	71
Figure 58 The concentration of Cu(II) ion in the feed phase and stripping phase at any time (Flow rate = 27 ml/h).....	71
Figure 59 The concentration of Cu(II) ion in the feed phase and stripping phase at any time (membrane thickness = 361.13 μm)	72
Figure 60 The concentration of Cu(II) ion in the feed phase and stripping phase at any time (membrane thickness = 497.48 μm)	72
Figure 61 The concentration of Cu(II) ion in the feed phase and stripping phase at any time (membrane thickness = 829.87 μm)	73

CHAPTER I

Introduction

At the present, various industrial activities such as mining, hydrometallurgy, electroplating, and circuit board processing, often discharge waste streams [1, 2]. The waste streams usually include effluent and catalyst [3] which may contain valuable heavy metals and toxic metals such as arsenic (As), lead (Pb), mercury (Hg), cadmium (Cd), chromium (Cr), copper (Cu), zinc (Zn), etc. The accumulation of heavy or toxic metals throughout the food chain leads to serious ecological and health problem [4]. Therefore, the motivations for metal recovery include not only meeting the strict regulation on effluent quality standards, but also the fact that some metals are expensive and can be reused [5]. Several techniques have been used for removal and recovery of heavy metal ions such as ion-exchange, chemical precipitation, adsorption, solvent extraction, membrane extraction, etc. [6]. These methods are suitable for different applications with their own limitations such as limited selectivity, high amount of extractant consumption, employing multiple steps, and high used cost [5]. Liquid membrane (LM) has been used for the removal and recovery of heavy metal ions [6] and for replacing purification step that could reduce the overall consumption of energy and the cost in industrial process [4].

LM technology is an efficient separation process which provides simultaneous extraction and stripping processes in the same stage where concentration of component is relatively low. In this process, selected components in the aqueous phase can be spontaneously transported through the membrane and re-extracted into the stripping phase which gives high selectivity and reduces separation or purification procedure [7]. Several advantages of LM include ease in conducting into a continuous flow system, uphill transport characteristic, and non-equilibrium

diffusion process governed by the kinetics of the membrane transport, etc. [5, 8]. The supported liquid membrane (SLM) is a non-dispersive type of LM. The membrane phase is immobilized in pores of a polymer supported by capillary forces. Thus, the amount of extractant required is small and expensive solvent can be used in SLM [6]. However, the main problem of LM is membrane instability due to leakage or losses of solvent during transport process and solubility of membrane phase in aqueous phases [8]. This work proposes the use of nanofibers layer as a support for the liquid membrane because nanofibers provide high porosity, high surface area-to-volume ratio, high mechanical strength, and flexibility in functionalization. In this work, polyvinylidene fluoride (PVDF) which is semi-crystalline polymer mostly used for hydrophobic membrane materials [9, 10], was fabricated into a sheet of nanofibers via electrospinning governed by the electrical forces [11].

Although the SLM has been applied in many fields in the past, the process is often limited by mass transport. In this work, this problem is overcome by using microchannel. Reactive extraction by nanofibers-supported liquid membrane (NSLM) was applied in a microchannel to recover heavy metal from wastewater. Copper was used as a model ion, while di-2-ethylhexyl phosphoric acid (D2EHPA) dissolved in kerosene was used as the extractant. The extractant was supported by a thin layer of polyvinylidene fluoride (PVDF) nanofibers to form a thin immiscible layer, i.e., liquid membrane, within the microchannel. The feed solution, CuSO_4 , was supplied on one side of the liquid membrane for copper extraction, while hydrochloric acid was supplied on the other side for stripping of copper ions from the liquid membrane. Effects of applied voltage during electrospinning, thickness of microchannel in microreactor, thickness of membrane, flow rates of both streams

and copper concentration in the feed stream on the extraction efficient were investigated and reported.

The objectives of this research included:

- To investigate the transport phenomena, reaction rate constant of reactive extraction by nanofibers-supported liquid membrane (NSLM) in microchannel.
- To investigate the effects of operating parameter on the efficiency of Cu(II) ions extraction.



CHAPTER II

THEORY AND LITERATURE REVIEWS

2.1 Liquid membrane (LM)

Membrane technology gradually becomes a popular separation technology over the past few decades [9]. Liquid membrane (LM) is the one of efficient membrane technology which can apply in many fields such as heavy metal removal and recovery process especially in cases when concentration of components is relatively low, wastewater treatment, gas separation, organic compound removal, drug recovery-separation, bio-separations, etc. In this process, targeted components or solutes in aqueous phase enhance permeability in comparison with solid membranes because diffusion in liquids is faster than diffusion in solids [12].

Liquid membrane (LM) technology is efficient separation process which can simultaneous extraction and stripping processes in the same stage. The thin layer of immiscible liquid as membrane phase is separated between two miscible liquid as feed phase and stripping phase. In this process, one or several components in the feed phase can be spontaneously transported through membrane and are re-extracted into the stripping phase, while other components are not which gets high selectivity and could reduce a separation or purification procedure [5, 7]. LM technology can be divided into 3 categories including bulk liquid membrane (BLM), supported liquid membrane (SLM), and emulsified liquid membranes (ELM) [8].

2.1.1 Bulk liquid membrane (BLM)

In bulk liquid membranes is consisted of the feed phase and the stripping phase which are directly separated by a thin layer of the immiscible liquid

as the membrane phase [13]. BLM is one of the uncomplicated forms of liquid membrane and simplicity to manipulate. However, the flux of BLM is low due to small specific interface area and long transportation path of components, so the mass transfer resistance increases. In addition, the use of large amount of organic solvents as liquids membrane phase increases capital cost in case of solvent loss, particularly when the solvents are expensive and instability in term of longtime performance [6].

2.1.2 Emulsion liquid membranes (ELM)

Emulsion liquid membrane is obtained by creating a water-in-oil emulsion which contains the extractant in the oil phase and the stripping agent in the internal aqueous phase [14]. The emulsion is dispersed in the aqueous phase which containing the components or solutes that transported through membrane into the stripping phase to be separated. The membrane separates the encapsulated internal droplets of the stripping phase in the emulsion from the external aqueous phase [1]. Some advantages of ELM including high flux due to high surface area per unit volume, low cost and energy consumption, and capability of treating of various compounds in industrial settling in a short time. However, the disadvantage is loss of extraction efficiency because the emulsion of the globules are lack of stability [12].

2.1.3 Supported liquid membranes (SLM)

Supported liquid membrane is a non-dispersive type of LM which have three-phase including feed phase, membrane phase and stripping phase [6]. The membrane phase is immobilized with immiscible organic solvent in the pores of a hydrophobic membrane by capillary forces and separates two miscible solution: feed phase (donor) and stripping phase (receiving) [8]. The targeted metal ions in feed phase are extracted with organic solvents at membrane interface as metal-

complex then diffusing across the membrane and are re-extracted to the other side of the membrane into the stripping phase. The mechanism of SLM process is showed in Figure 1.

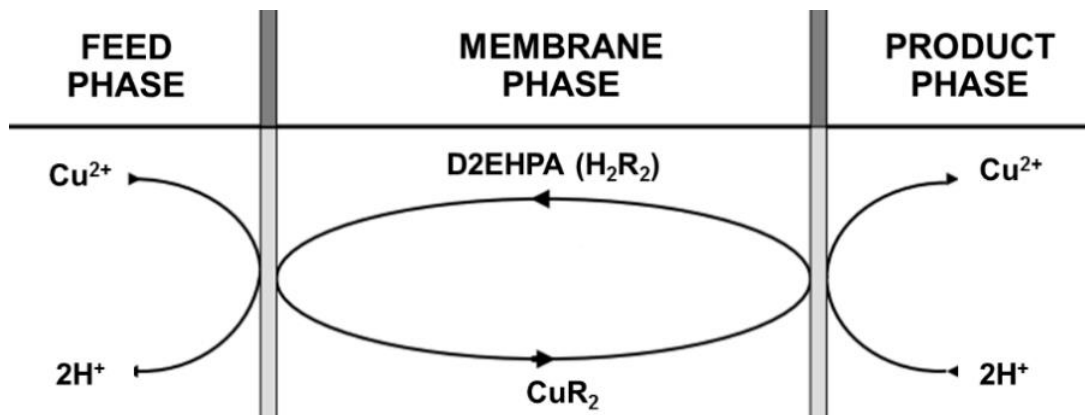


Figure 1 Facilitated transport of Cu^{2+} through liquid membranes using a carrier mediated co-transport mechanism.

The thin layer of membrane can be configured either as a flat sheet or cylindrical type which can be categorized namely, flat sheet supported liquid membrane (FSSLM) and hollow fiber supported liquid membrane (HFSLM), respectively[6]. As for FSSLM, the solid support membrane is immobilized with extractant and is clamped between feed and stripping phase which showed in figure 2 [6]. Both phases are stirred by mechanical stirrers. As for HFSLM, the shell side have many thin fibers which are packed in neat rows which showed in figure 3 [15] and the feed phase solution is pumped through the fiber whereas the stripping phase solution pass through the shell side [15]. Although this module provides highest surface area per volume ratios but difficult to build-up and expensive module.

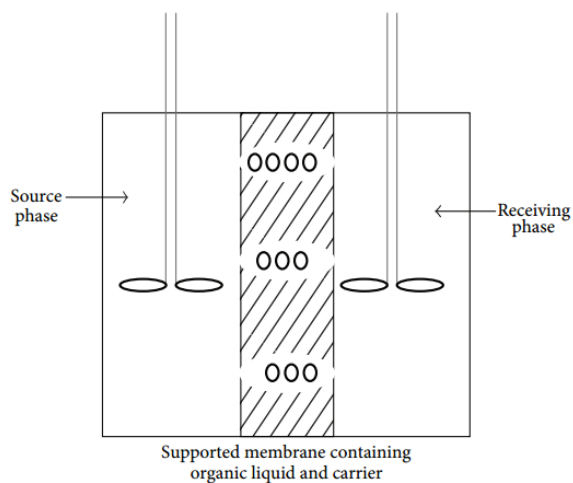


Figure 2 Schematic diagram of flat sheet supported liquid membrane (FSSLM) in membrane separation process

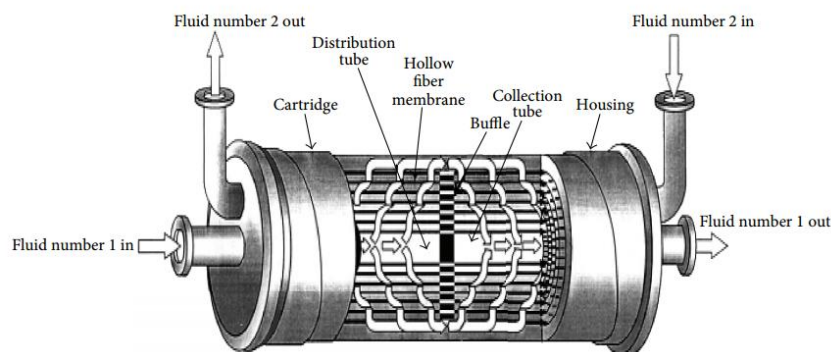


Figure 3 Hollow fiber supported liquid membranes (HFSLM)

2.1.4 The components used in Liquid Membrane

During the process of liquid membrane, the properties of the membrane have a great influence on efficiency and selectivity. Thus, the materials of LM such as supports membrane, extractant or carrier and diluent are briefly reviewed in the following sections. The extractant is responsible for LM properties in terms of permeability and selectivity, while the support affects the permeability by its porosity. [12]

(i) **Support membrane:** the solid support in LM is usually a hydrophobic polymer which plays an active role in the transport and extraction efficiency [16] and also provides a structural support for the membrane phase so that it could maintain the extractant solution in the membrane pores by capillary force [6]. The selection of the polymeric support has a great influence on the performance, stability and lifetime of the liquid membrane. Thus, it is very significant to select the type of materials and support structures for suitable applications. The polymeric support required should be highly hydrophobic, have small pore size, high porosity, chemically and thermally stable on contact to the solution in both phases and organic solvent because it contact directly interface of the support membrane [8].

Among various hydrophobic polymers, the most frequently used membrane materials are polypropylene (PP), polytetrafluoroethylene (PTFE) and polyethylene (PE). However, the relatively low porosity of PP and PTFE membranes that produced by stretching or thermal methods affect to restrict the amount of extractant absorption [10]. Another strong hydrophobic polymer, polyvinylidene fluoride (PVDF) has been successfully employed for making membranes due to excellent chemical and thermal resistances which makes them stable in most of the corrosive chemicals and organic compound [12]. The table 1 showed previous research of material support for supported liquid membrane process. In this work, polyvinylidene fluoride (PVDF) was used as a support membrane, which will be discussed in the next section.

Table 1 Literature review of material support for SLM process

Support Material	Module	Process	Ref
Polypropylene (PP)	Hollow fiber	Separation of mercury (II) from petroleum produced	[6]
Polypropylene (PP)	Hollow fiber	Separation of Cu and Zn ions by HFSLM containing LIX84 and PC-88A	[17]
Microporous hydrophilic (PVDF)	Flat sheet	Heavy metal ions extraction using SLM containing ionic liquid as carrier	[4]
Polyvinylidene fluoride (PVDF)	Hollow fiber	Mass transfer of Copper (II) in HFRLM with different carriers	[5]
Polytetrafluoroethylene (PTFE)	Flat sheet	Big carrousel mechanism of copper removal from ammonical wastewater through SLM	[18]
Polytetrafluoroethylene (PTFE)	Flat sheet	Pertraction of l-lysine by SLM using D2EHPA/M2EHPA	[19]

(ii) **Extractant or carriers:** the extractant used for SLM process is basically an organic solvent which has been chosen based on solubility of the target components present in the feed phases. The high solubility of the extractant causes the high mass transfers [6]. The organic solvent is immobilized in the solid support pore and acts as a membrane phase [2]. Table 2 shows different compositions and conditions of LM on copper removal. The different extractant affects the transport properties such as mass transfer flux and separation efficiency. Thus, the used of organic solvent should be considered for suitable with applications. Firstly, the organic solvent should be hydrophobic enough to ensure immiscibility with aqueous phases. Secondly, the solvent should be characterized by low viscosity, which results in high mass transfer through the membrane. However, the low viscosity decreases

membrane stability. The other important factor is solvent volatility, which should be low to keep the membrane phase in the pores of the support [8].

Table 2 Compositions and conditions of LM on copper removal

Metal	Extractant	Diluent	Stripping	Method	Ref.
Copper	D2EHPA	Kerosene	CuSO ₄ and Disodium salt	ELM	[20]
Copper	D2EHPA	Hexane Heptane	H ₂ SO ₄	ELM	[21]
Copper	D2EHPA	Kerosene	H ₂ SO ₄ /HCl	PIM	[22]
Copper	D2EHPA	Kerosene	HCl	HFSLM	[2]
Copper	LIX984N	Kerosene	H ₂ SO ₄	HFSELM	[7]
Copper	LIX54	Kerosene	H ₂ SO ₄	SLM	[18]

(iii) **Diluents:** The diluents are generally used for preparation of various concentrations of the organic extractants used for the extraction of the metal ions. The nature of the diluents preferred is the same as it is for the solvent extraction process and so the diluents should have high dielectric constant, low viscosity, cheap, and so forth. However, the primary requirements in the membrane formulation are to lower the solvent viscosity which leads to the diffusivity of the solute complex within the membrane. The effect of the diluents is quite significant on the extraction of metals because both physical and chemical interactions exist in between diluent and extractant. The diluents, namely, kerosene, xylene, toluene, hexane, cyclohexane, and so forth, are generally used in hydrometallurgical processes [23].

2.1.5 The transport of heavy metal ions through liquid membrane

The transport of Cu(II) ions from the feed phase through nanofibers supported liquid membrane to stripping phase in microchannel is coupled counter-transport. The driving force is the difference in concentration of the metal ion between the phases. The six step of mass transfer in the SLM process are following in figure 4:

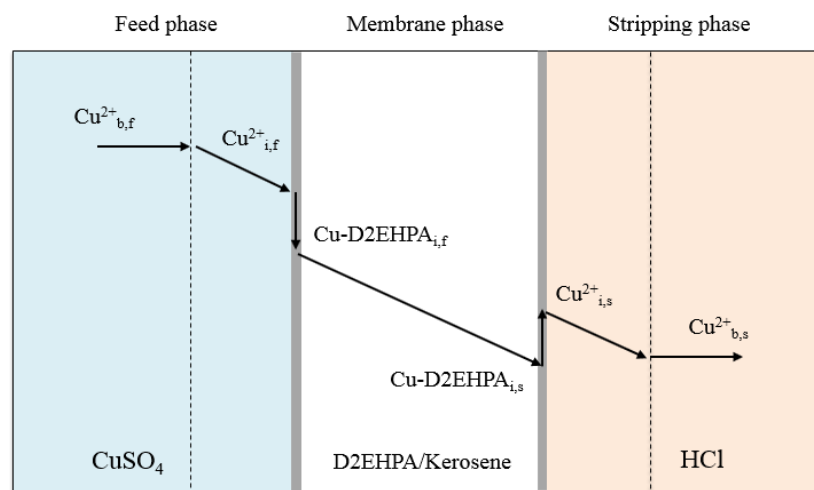


Figure 4 Transport mechanism of the Cu(II) ions

- (i) The Cu(II) ions from the bulk of feed phase ($\text{Cu}^{2+}_{b,f}$) diffuse to the feed-interface of membrane.
- (ii) The complexation reaction occurs at feed-interface of membrane which Cu(II) ions react with extractant solution (H_2R_2 represents the dimeric form of D2EHPA dissolve in kerosene) forming to Cu-D2EHPA complexes. The structures of Cu(II) complex is showed in figure 5. The reaction mechanism can be described as follows: eq. (1) [24] where (aq) represents the species in the aqueous phase and (org) represents the species in the liquid membrane phase.



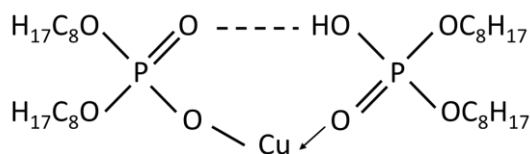


Figure 5 Copper (II) complex structure

- (iii) The Cu-D2EHPA complexes diffuse across membrane phase from feed-interface to stripping-interface of membrane.
 - (iv) The decomplexation reaction occurs at stripping-interface of membrane which Cu-D2EHPA complexes react with hydrogen ions from the hydrochloric solution (HCl) forming to Copper(II) chloride (CuCl₂) in the stripping solution. The reaction mechanism can be described as follows: eq. (2) [24]
- $$\text{CuR}_2 (\text{org}) + 2\text{H}^+ (\text{aq}) \rightarrow \text{Cu}^{2+} (\text{aq}) + \text{H}_2\text{R}_2 (\text{org}) \quad (2)$$
- (v) The Cu(II) ions from stripping-interface of membrane diffuse to the bulk of stripping phase.
 - (vi) The regenerated carriers diffuse through membrane from stripping-interface to feed-interface of membrane.

2.1.6 The advantages and disadvantages of support liquid membrane

Successful applications of SLM are possible due to their advantages compared to other separation methods. The main advantages of SLM are following:

- (i) The SLM process can simultaneous extraction and stripping in the same stage. The combinations could reduce the size of reactors, resulting in reduced energy consumption and investment cost [6].
- (ii) The liquid membrane in SLM selects one or several components in the aqueous phase can transport spontaneously through the membrane while

other components are not which gets high selectivity and could reduce a separation or purification procedure [7].

- (iii) The characteristic of transport in SLM is uphill transport. In conventional method the separation is limited by equilibrium conditions but SLM acts on nonequilibrium mass transfer characteristic which the target components can be spontaneously transport from low to high concentration solution [5, 8].
- (iv) The SLM of hollow fiber module type provide high interfacial area per unit volume, resulting in reduced the required equipment volume [25].
- (v) The SLM process is a nondispersive type of LM that the organic solvents as membrane phase is immobilized in the pores of a polymer by capillary forces. The amount of organic solvents required are small, so the expensive solvents can be used for SLM. Moreover, there is less solubility of the organic solvent in aqueous phase, so the solvent loss is much less [6].

Despite the SLM has been applied in many filed due to several advantage. There are some problems limiting in the process. The main problems are of SLM are following:

- (i) The stability of the liquid membrane in term of long-time performance, caused by leakage, losses, evaporation or dissolution of organic solvent as membrane phase during transport process leads to reduce mass transfer flux, efficiency and selectivity [26].
- (ii) The thicker layer of membrane phase affect to increase the mass transfer resistance [6].
- (iii) The SLM process is a new technology and lack of research.

2.1.7 The effect of various parameters on the liquid membrane (LM) extraction process

There are several operating parameters that influence the removal or recovery metal ions on liquid membrane extraction process, as listed in the following.

(i) The effect of extractant concentration

The extractant concentration is one important factor for extraction process. In the liquid membrane extraction process, the metal ions in the aqueous phase react with carriers in the membrane phase and then form to metal-complexes which can transport through membrane and re-extract in the stripping phase. Previous studies [5] showed that there is almost no mass transport of metal ions when the membrane without a carrier which means that there is no facilitated transport. It indicates that the extractant had significant effect on the transport of metal ions across the membrane. The mass transfer flux depends on the facilitated transport capacity of the carrier in membrane phase. Weidong Z. et al. [2] studied the transport of Cu(II) through hollow fiber supported liquid membrane. The influence of the carrier concentration was investigated. It was reported that, the higher carrier concentration facilitates mass transfer process resulting in higher distribution coefficient and increases the mass transfers driving force. Therefore, the rate of complex reaction and the mass transfer flux are higher. Kavitha N. et al. [22] observed that the flux of Cu(II) linearly increases with increasing carrier concentration and then slightly decrease (Figure 6) [22]. The increasing of carrier concentration increases the formation of metal-complexes and also increases the concentration gradient along the thickness of membrane. However, the carrier concentration is too high results in high viscosity in the membrane phase which limits diffusion of metal-complex through the membrane [27, 28]. Alguacil F.J. et al. [28] reported that as for

the low carrier concentration, the rate-determining step is the diffusion of metal-complexes across the membrane whereas high carrier concentration, the rate-determining step is the diffusion of metal ions from bulk to interface of membrane.

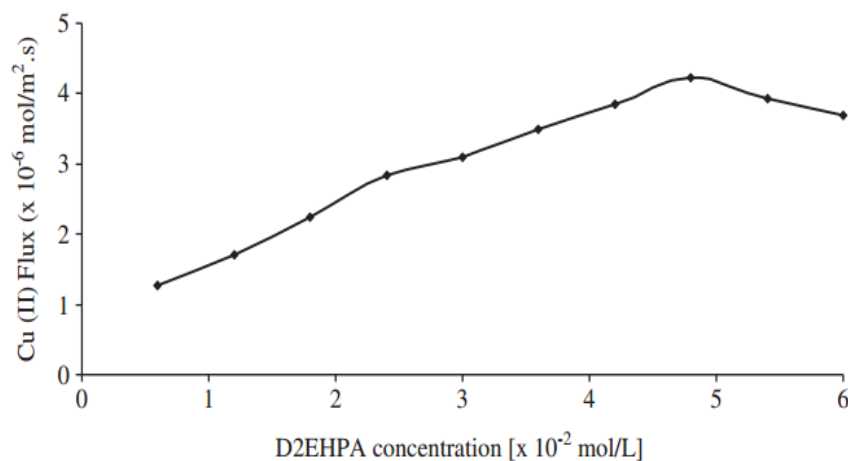


Figure 6 Effect of D2EHPA concentration in membrane phase of Cu(II) flux.
(Experimental conditions: feed phase: 15.7×10^{-4} mol/L; strip phase: 1 M H_2SO_4)

(ii) The effect of initial metal concentration in the feed phase

The feed concentration is another important factor in the extraction process. Kavitha N. et al. [22] studied the recovery of Cu(II) through polymer inclusion membrane with di (2-ethylhexyl) phosphoric acid as carrier from e-waste. The results showed that the complexation rate at interface of membrane increases with increasing of Cu(II) concentration. At lower Cu(II) concentrations, the initial flux is a strong function of the initial Cu(II) concentration. Thus, the permeation process is controlled by diffusion of Cu(II) species in the lower range of concentration [29]. In term of high concentrations, the flux of metal ions is constant (Figure 7) [22], probably due to the saturation of membrane pore with metal-complex and buildup of the carrier layer on the interface of membrane resulting in lower effective membrane area [29]. Similar to the study by Kocherginsky N.M. et al. [18], they

reported that the rate limiting step is determined by the diffusion of copper ions in the stagnant aqueous layer with lower concentration than 0.1 M. In addition to, the flux reaches maximum with higher concentrations more than 0.1 M due to the liquid membrane and the pore liquid are saturated by the metal-carrier complex molecules [30, 31]. Therefore, the transport is limited by the diffusion of metal-complexes through the membrane phase. Ren Z. et al.[32] reported that the overall mass transfer coefficient decreases, whereas the resistance of de-complexation at the stripping interface increases with increasing initial copper concentration in the feed phase.

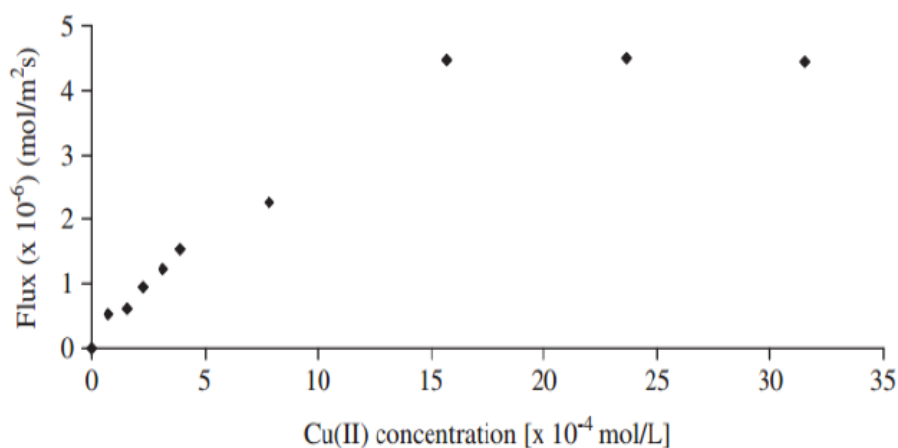


Figure 7 Effect of initial Cu(II) concentration on the transport flux. (Experimental conditions: strip phase: 1 M H₂SO₄; D2EHPA concentration in PIM: 4.8×10^{-2} mol/L.)

(iii) The effect of stripping phase concentration

In SLM process, the extraction step occurs at the interface between the feed and membrane phase which requires a simultaneous re-extraction step at the opposite side of the membrane to achieve overall of the transport process [22]. In the re-extraction stage, the extractant is regenerated and the metal is stripped to stripping phase. If the metal complex is not completely stripped, the membrane

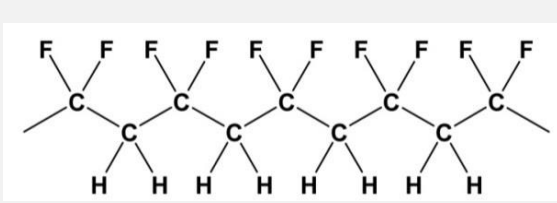
phase becomes saturated with the complex and the permeation rate may decrease [33]. Therefore, the concentration of the stripping phase also influences on the mass transport. Huidong Z. et al. [7] studied the recovery of copper ions from wastewater by hollow fiber supported emulsion liquid membrane. The results showed that, the mass transfer rate is accelerated with increasing H^+ concentration in the stripping phase (less than or equal to 5 mol/L) due to higher concentration improves copper complex dissociation and maintains the carrier concentration at higher level. However, the mass transfer rate increases slowly when high H^+ concentration. Similar to the study by Kavitha N. et al [22], the results showed that increasing the H_2SO_4 concentration, the flux of Cu(II) increase and no effect on the transport rate with higher concentration above 1 mol/L. In addition to the stripping concentration, the type of stripping solution has influence on the re-extraction. Ren Z. et al. [24] reported that the using HCl acts as stripping solution for copper removal, Cl^- greatly affects the re-extraction and gets the maximum distribution coefficient when the concentration of HCl is around 6 mol/L. Moreover, the ability to re-extraction copper(II) complex from the membrane phase with same concentration is $HCl > H_2SO_4 > H_3PO_4$.

2.2 Poly (vinylidene fluoride) (PVDF)

The membrane is the key of the membrane separation technology, and it directly affects efficiency of process [9]. The organic polymers are widely used as membrane such as polymers include polyacrylonitrile (PAN), polysulfone (PSF), polyamide, poly(ether sulfone) (PES), polyimide, polytetrafluoroethylene (PTFE), and poly(vinylidene fluoride) (PVDF) [10]. PVDF is one of the most used membrane materials and has been paid much attention by researchers and manufacturers in recent years [34].

Poly (vinylidene fluoride) (PVDF) is semi-crystalline polymer, consisting of the repeated monomer unit $-(CH_2CF_2)_n-$ [3 5] which the crystalline phase provides mechanical strength, impact resistance and thermal stability as well as excellent aging resistance while the amorphous phase offers flexibility [10]. Thus, PVDF was used in various applications requiring strength, the highest purity, and stable when attacked by corrosive chemicals and organic compounds including acids and oxidants [11]. PVDF is soluble in common organic solvents such N,N-dimethyl acetamide (DMAc), N-methyl-2-pyrrolidone (NMP), and N,N-dimethyl formamide (DMF) [9]. The PVDF membranes can be fabricated by conventional non-solvent induced phase separation (NIPS) process, thermally induced phase separation (TIPS), vapor induced phase separation (VIPS), solution casting, electro-spinning, etc. [9] which could be prepared as membrane in many types such as powder, flat sheet, hollow-fiber or tubular pipe, etc. [11] The physical properties of PVDF are shown in Table 3

Table 3 The physical properties of PVDF

PROPERTIES	DATA
CHEMICAL STRUCTURE	 <p>The diagram shows a segment of the PVDF polymer chain. It consists of a backbone of carbon atoms. Each carbon atom in the backbone is bonded to two other carbon atoms. The first carbon in the segment is bonded to two fluorine (F) atoms. The second carbon is bonded to two hydrogen (H) atoms. This pattern repeats: the third carbon has two fluorine atoms, the fourth has two hydrogen atoms, and so on. The chain ends with single bonds extending from the first and last carbon atoms, indicating it is a repeating unit.</p>
MOLECULAR FORMULA	$(CH_2CF_2)_n$
MOLECULAR WEIGHT	Average Mn ~107,000, Average Mw ~275,000 by GPC
MELTING POINT	166-170 °C
VAPOR PRESSURE	15 mmHg (32 °C)
DENSITY	1.78 g/mL at 25 °C
SOLUBILITY	Some polar solvents such as organic esters and amines
SYNONYMS	Polyvinylidene difluoride; poly(vinylene fluoride); Kynar; Hylar; Solef; Sygef; poly(1,1-difluoroethane)

2.3 Electrospinning process

Nanofibers are fibers with diameters in the nanometer range which can be generated from different polymers and hence have different physical properties and application potentials. Previous study [11] found that the properties of the fiber improve with decreased diameter which nano-scale of fiber provides high porosity, high surface to volume ratio, mechanical strength, and flexibility in functionalization. There are many different methods to produce nanofibers such as electrospinning, phase inversion technique, non-solvent induced phase separation (NIPS), solution casting, etc. [9]. Electrospinning is the most commonly used method to generate nanofibers due to its many advantages such as, simplicity of process, control of fiber morphology and dimension, repeatability and low cost, etc. [11]

Electrospinning is a process which governed by the electrical forces to produce polymer fibers with diameters ranging from 2 nanometers to several micrometers [36]. The instruments necessary for electrospinning is consisting of a syringe connected with a needle to contain the polymer solution, two electrodes, a direct current (DC) high voltage supply in the kV range and collector sieve plate. The setup of electrospinning process shows in Figure 8. An DC electric field is applied between the droplet and a grounded collector sieve plate, overcomes the surface tension, a thin jet is formed. The jet of the charged solution is accelerated towards the collector and polymeric fibers randomly deposit on the collector surface [11]. Over time, these nanofibers is a non-woven network that can be used as a supported membrane [37]. Table 4 showed overview about various parameters on electrospinning and their effects on fiber morphology.

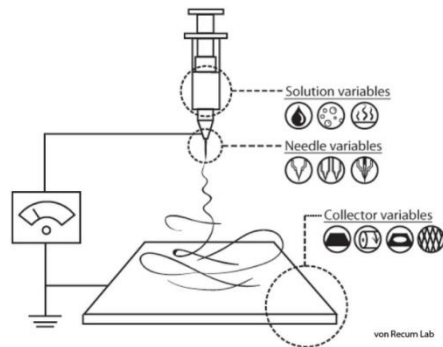


Figure 8 Electrospinning schematic formation by electrospinning

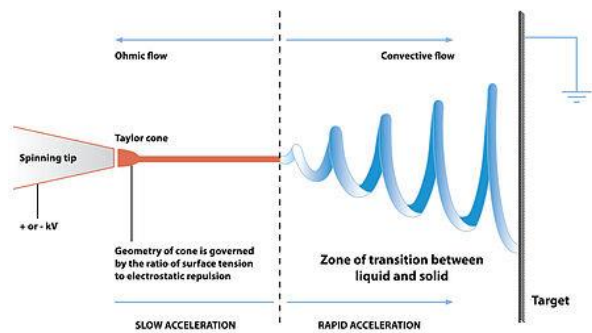


Figure 9 Diagram showing fiber formation by electrospinning

Table 4 Electrospinning parameters and their effects on fiber morphology

Parameters	Effect on fiber morphology
Viscosity of polymer solution	Low - beads generation High - increase in fiber diameter, disappearance of beads
Concentration of Polymer	Increase in fiber diameter with increase of concentration
Applied voltage	Decrease in fiber diameter with increase in voltage
Feed rate	Decrease in fiber diameter with decrease in flow rate, generation of beads with too high flow rate
Distance between tip and collector	Generation of beads with too small and too large distance, minimum distance required for uniform fibers
Humidity	High humidity results in circular pores on the fibers.

2.4 Microreactor

The microreactor technology has attracted a great deal of attention as an enabling tool for novel reaction development and scale-up. Microreactors have helped to minimize reagent consumption and energy waste due to their small dimensions, which in most cases do not exceed 1 millimeter and greater than 1 micron in at least one dimension [38]. The use of microreactor devices make it possible for synthetic chemists and process engineers to perform reactions with an unprecedented control over mixing, mass- and heat-transfer, safety, reaction residence time and other process parameters, which results in enhanced reproducibility. In addition to, the reaction rates can be accelerated by orders of magnitude and the reaction times shrink from hours to minutes and seconds.

The advantages of microchannel are high surface-to-volume ratio, quick and effective mixing of the reagents, more effective heat transfer and mass transfer comparing to the classical chemical reactors, short reaction time, very small reagent quantities used for the synthesis (which is quite important for reaction optimization), the regulation of the main reaction parameters (flow rate, residence time, pressure, temperature) with very high accuracy, the simple and quick adjustment of optimal reaction conditions.

CHAPTER III EXPERIMENTALS

3.1 Reagent

Di-2-ethylhexyl phosphoric acid (D2EHPA, purity >97%) and polyvinylidene fluoride (PVDF, average Mw ~180,000 measured by gel permeation chromatography) were obtained from Sigma Aldrich. N,N-dimethylformamide (DMF) and hydrochloric acid (HCl, purity 37%) were provided by QReC (grade AR). Kerosene (99%) was provided from BDH. Cupric sulfate ($\text{CuSO}_4 \cdot 5\text{H}_2\text{O}$) was supplied from Ajax Finechem Pty Ltd. All chemical reagents were used without further purification.

3.2 Apparatus

The microreactor setup (figure 10) is consisted of acrylic plates, teflon sheets and sieve plate of membrane.

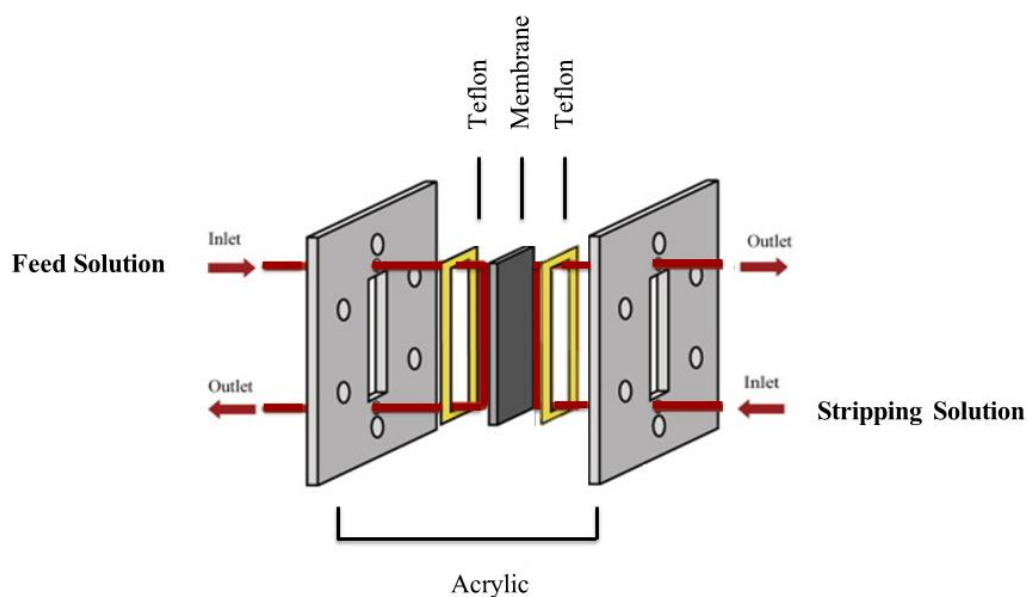


Figure 10 The components of microreactor

3.2.1 Acrylic plates

Acrylic plates are available to hold the structure of the reactor consisting of top and bottom plate. Both sides of acrylic plates have two holes of one inlet and one outlet. The dimension of acrylic plates are 11 cm x 15 cm and the thickness is 1.5 cm. The photograph of acrylic plates is shown in figure 11.

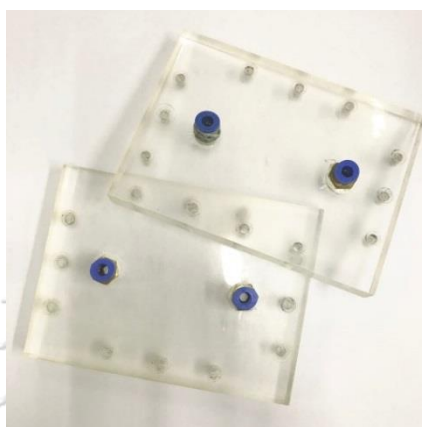


Figure 11 Acrylic plates

3.2.2 Teflon sheets

Teflon sheets from Scientific commodities inc. (SCI) are available to make the hexagonal microchannel consists of two sheets for feed and stripping channels. The teflon thickness is equal to in the range of 125-500 μm and the dimension of teflon sheet is 10 x 2.5 cm. The average volume of both side of microchannel is in the range of 0.3–1.2 ml. The photograph of teflon sheets is shown in figure 12.



Figure 12 Teflon sheets

3.2.3 Collector Sieve plate

The fibers of PVDF solution are deposited on collector sieve plate which conducts as membrane phase and separates between feed phase and stripping phase. The particle size of sieve plate is 400 mesh. The dimension of sieve plate is 11 x 3.5 cm. The photograph of collector sieve plate is shown in figure 13.



Figure 13 Collector Sieve plate

3.3 Fabrication of PVDF nanofibers membrane

A flat sheet of PVDF nanofibers was used as the membrane support polymer which was self-manufactured by a typical electrospinning method at room temperature. The 15 %wt. of PVDF (average $M_w \sim 180,000$ by GPC) was dissolved in a mixed solvent of N,N- dimethylformamide (DMF) and kerosene (1:1 v/v ratio) in a beaker and then stirred for 45 minute at 60 °C until a homogeneous solution was formed. The electrospinning setup (figure 14) consists of a high voltage power supply, a syringe with metal needle, a syringe pump, and a conductive collector. The PVDF solution was loaded into the syringe connected to a power supply to establish a charged polymer jet. The nanofibers products were deposited on a sieve plate (400 mesh) which dimension is 11 x 3.5 cm. The parameters for electrospinning process were as follows: 15-20 kV of applied high voltage; flow rate of 2.5 mL/h; the distance between needle of syringe and sieve plate of 12 cm.

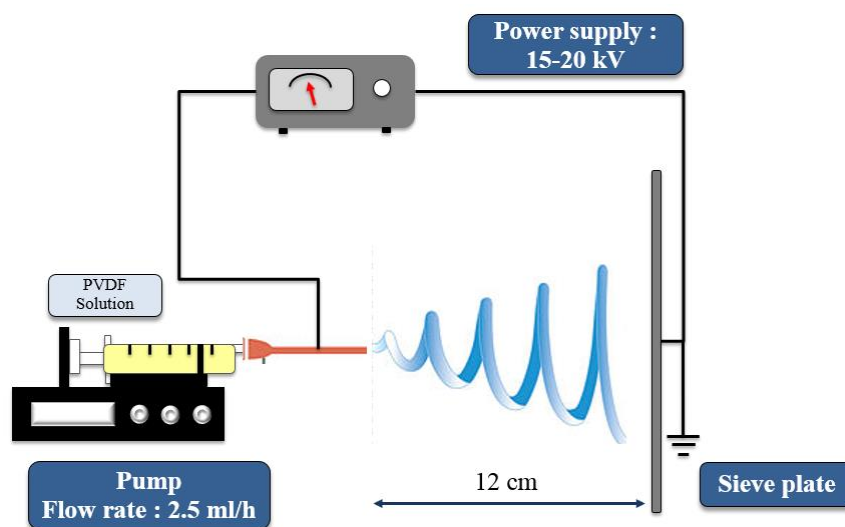


Figure 14 The experimental set up of PVDF nanofibers membrane synthesis by electrospinning method

3.4 Experimental procedures

Before being assembled into the microreactor, the PVDF nanofibers membrane was impregnated with a solution of D2EHPA in kerosene (1:1, v/v) for 20 minutes to ensure that all membrane pores were filled with solution. The membrane was then assembled by placing it between two Teflon sheets. The components of the microreactor are shown in figure 11. The feed (CuSO_4 aqueous solution) and stripping solution (6 M, HCl in water) were loaded in separated syringes, which were connected to the microreactor. The pump was used to control the flow rate which the flow of the feed and the stripping solution was counter-current.

3.5 Analysis

3.5.1 Ultraviolet-visible spectrophotometer (UV-Vis)

The samples of product from the microchannel were periodically taken from the feed and stripping outlet every 20 minutes to be measured the concentration of Cu(II) ion by the colorimetric method of UV-Vis which is shown in figure 15 and using

quartz as cuvette. The scanning was commenced at wavenumber ranging from 200 - 900 nanometers and detect wavelength of Cu(II) ion at 860 nanometers. The photograph of UV-Vis is shown in **Figure 15**.



Figure 15 UV-Visible spectrophotometer

The efficiency of Cu(II) extraction from the feed phase (EE) and Cu(II) stripping in stripping phase (SE) were calculated using equation 3 and 4 respectively.

$$EE (\%) = \frac{C_{fo} - C_{ft}}{C_{fo}} \times 100 \quad (3)$$

$$SE (\%) = \frac{C_{st}}{C_{fo} - C_{ft}} \times 100 \quad (4)$$

Where C_{fo} is the initial concentration of Cu(II) in the feed phase and C_{ft} , C_{st} are the concentration in the feed phase and stripping phase at any time.

3.5.2 Scanning electron microscope (SEM).

The surface morphology of PVDF nanofibers membrane was observed by field emission scanning electron microscope (FE-SEM) at 10 kV.

3.5.3 Total organic carbon (TOC)

Total Organic Carbon (TOC) analyzer is commonly used to quantify the amounts of organic carbon. In this work, the PVDF nanofibers membrane was impregnated with a solution of D2EHPA in kerosene. To test the leakage of extractant from membrane phase in the microchannel, this instrument is used to detect the solution outlet from microchannel reactor, measured as carbon concentration. The temperature used to analysis of the TOC is 680 °C. The photograph of TOC analyzer (Shimadzu, TOC – V CHP) is shown in **Figure 16**.



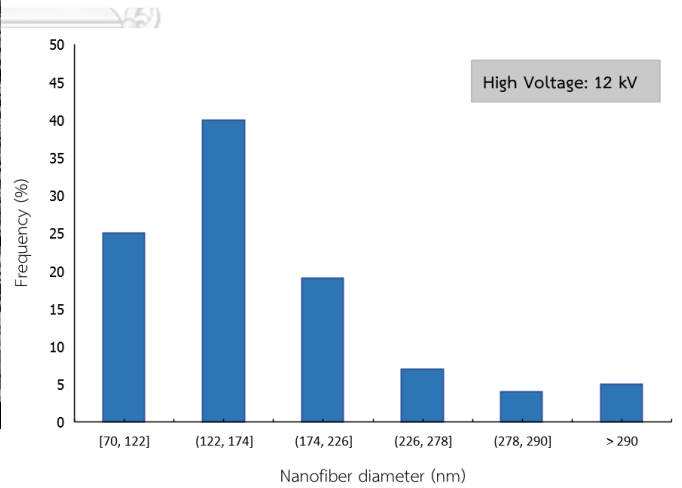
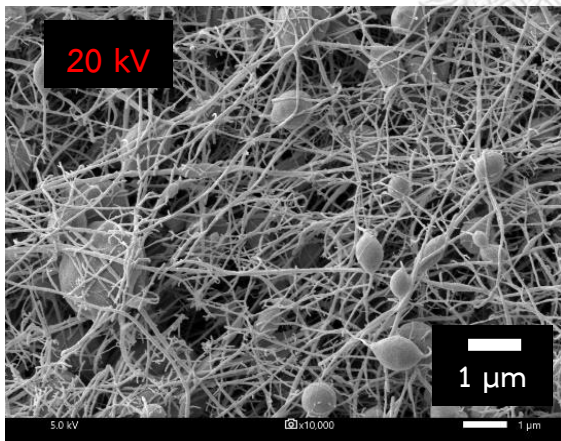
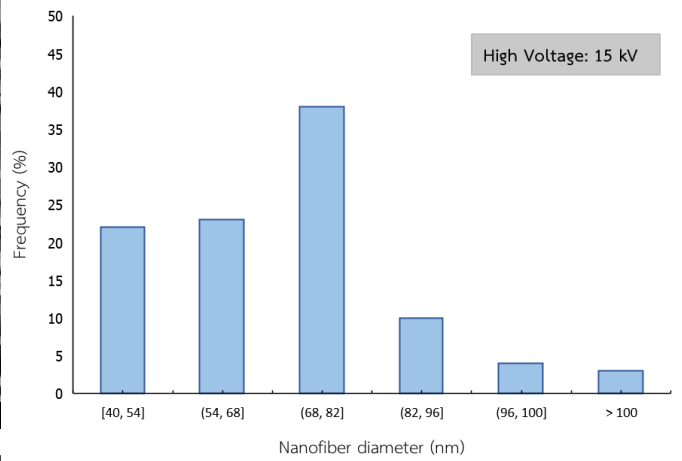
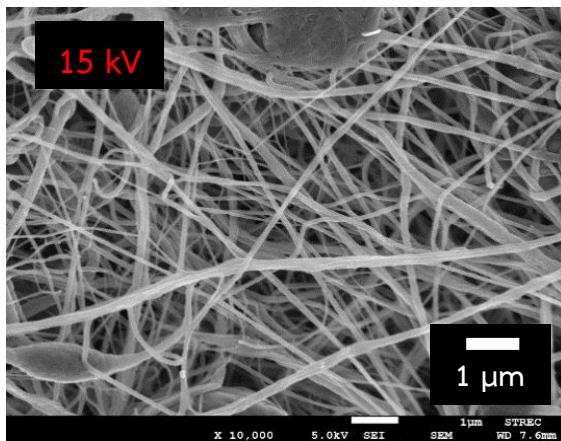
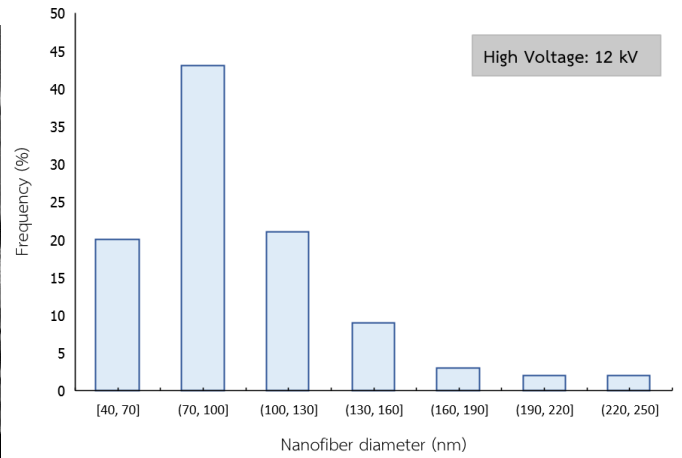
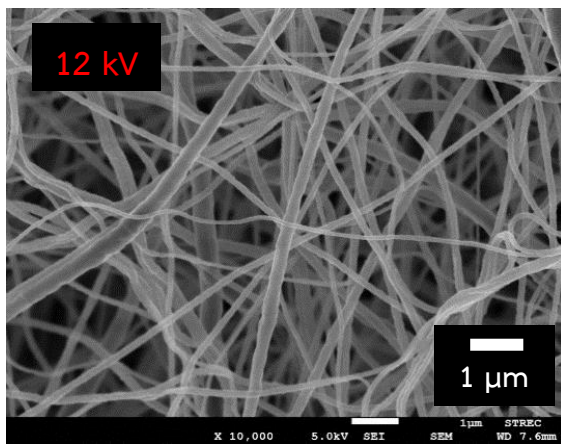
Figure 16 The photograph of TOC analyzer

CHAPTER IV

RESULTS AND DISCUSSION

4.1 The surface morphology of PVDF nanofibers membrane

Figure 17(a) shows FE-SEM images of PVDF nanofibers membrane that were successfully prepared with random interconnected structure by electrospinning method, resulting in pore structure between the nanofiber. This unique pore structure is beneficial to entrap and retain organic solvent as extractant effectively, and it facilitates the metal ion to diffuse smoothly across the membrane. Photoruler software was used to determine the nanofiber diameters, by measuring at least 100 fibers. In this study, the applied high voltage was conducted under 12, 15 and 20 kV, resulting in PVDF nanofibers with average diameter of 170, 100, and 70 nm, respectively. The nanofiber diameter histograms are also given in Figure 17(b). Higher applied voltage results in reduction of the fiber diameter due to greater of the solution with the greater columbic forces in the jet as well as a stronger electricfield [11]. However, when the voltage is too high, it results in broken fibers and apparent of beaded fibers. Although the fiber diameter is different but not significant on the process because the PVDF nanofiber membrane is impregnated with a large amount of extractant solution Thus, the membrane was immersed in the extractant solution as a layer instead of sticking on the fiber.



(a)

(b)

Figure 17 (a) FE-SEM images of electrospinning PVDF nanofibers membranes (b) The nanofiber diameter histograms

Then, the synthesized PVDF nanofiber membrane under 15 kV of the applied high voltage was impregnated with pure kerosene to test the leakage of extractant from membrane phase in the microchannel. Kerosene was used as diluent because of low the polarity solvent resulting in weak solvation effect so the effective concentration of extractant may not be reduced. One side of microchannel was fed with a CuSO_4 solution and the other side was fed with HCl solution where the flow of solution is counter-current. The both solution outlet from microchannel reactor was characterized to determine amount of kerosene by total organic carbon analyzer. The results show that only 0.38% of impregnated kerosene leaks out from the membrane within 160 minutes of operation. Because the PVDF nanofiber membrane is highly hydrophobic and lipophilic, it can retain kerosene. Hence, it is suitable to be used as a supported for liquid membrane. Moreover, Cu(II) ion was barely detected on the stripping phase, indicating that kerosene does not allow direct diffusion of Cu(II) ion through the membrane phase [5].

4.2 The reactive extraction of metal ion

In this part, only reactive extraction is considered. Hence, the system investigated was a microchannel consisting of 2 phases: feed phase and membrane phase. One side of microchannel was fed with a CuSO_4 solution and the other side was fed with D2EHPA/Kerosene solution where the flow of solution was counter-current and nanofiber membrane was placed between the feed phase and the membrane phase. This reaction occurred at feed/membrane interface where Cu(II) ions reacted with extractant solution in the membrane phase (D2EHPA dissolve in kerosene) forming to Cu-D2EHPA complexes and transferred to membrane phase. Then, the nanofiber membrane was replaced with fresh membrane phase and continued to react with the fresh feed phase. The reaction mechanism can be

described as follows: eq. (1) [24]. The effect of microchannel thickness and flow rate of solution were discussed.



where H_2R_2 represents D2EHPA/Kerosene, CuR_2 represents Cu-D2EHPA complex, (aq) represents the species in the aqueous phase, (org) represents the species in the liquid membrane phase.

4.2.1 Effect of microchannel thickness on reactive extraction

The influence of microchannel thickness on reactive extraction of metal ions was studied by varying the thickness of teflon on each side to be 175, 300, and 425 μm . As the height of the microchannel was increased, the flow rates of the solutions were adjusted to 10, 18, and 23 mL/h, respectively to keep the mean residence time constant at 133 sec. For all experiment, the initial concentration of Cu(II) ion solution was equal to 1 g/L with a solution of D2EHPA in kerosene (1:1, v/v). The samples of product were periodically taken from the both outlet microchannel every 20 minutes to be measured the concentration of Cu(II) ion by UV-vis. Table 5 shows the concentration of Cu(II) ion at steady state and rate of reactive extraction with different thickness of microchannel. The results confirmed that microchannel thickness affected on reactive extraction efficiency. Because of continuous process, so the Cu(II) ion in solution diffuses from bulk to feed/membrane interface and also blow to output by convection. As for the small thickness of microchannel, the concentration of Cu(II) ion at steady state in feed phase was lower because Cu(II) ion can be extracted more. The small diffusion distance in microchannel improves effective mixing of the solution by diffusion which occurs very quickly and also increases surface area to volume ratio of microreactor [39] led to enhance the

mass transfer rate due to convection and renews the interface between the two phases, as shown in figure 18. Moreover, the concentration gradient across membrane increases improving the diffusion of metal ions through membrane [40]. On the other hand, the results showed that the concentration of Cu(II) ion at steady state in membrane phase was lower when decreased the thickness of microchannel probably due to the saturation of membrane pore with metal-complex and buildup of the carrier layer on the interface of membrane resulting in lower effective membrane area [29] and less fresh membrane phase to replace in nanofiber membrane. The data of Cu(II) ion concentration at steady state in feed phase was determined the extraction efficient according to equation (3) which is shown in figure 19. The results showed that the extraction efficiency slightly increased with decreasing the thickness of microchannel, which was 88.61%, 77.50% and 77.22% according to 175, 300 and 425 μm of microchannel thickness. This result corresponds to the data from table 5. However, the extraction efficiency of Cu(II) ion does not change significantly as the thickness of microchannel decreased from 425 μm to 175 μm , indicating that the mass transfer from bulk to interface of membrane is not the rate determining step in the reactive extraction process. Thus, concluded that the using microchannel for reactive extraction of metal ion can overcome limited of mass transfer.

Table 5 The outlet concentration of Cu(II) ion at different microchannel thickness on the reactive extraction

Thickness of microchannel (μm)	Concentration of Cu(II) ion in feed phase (mg/L)	Concentration of Cu-D2EHPA in membrane phase (mg/L)	Rate of reaction ($\text{mol/L}\cdot\text{s}$)
175	114.52	1487.59	7.54×10^{-5}
300	226.27	1881.80	5.75×10^{-5}
425	240.27	2004.58	5.55×10^{-5}

(1) Concentration measures at steady state (2) Initial concentration of Cu(II) ion: 1000 mg/L

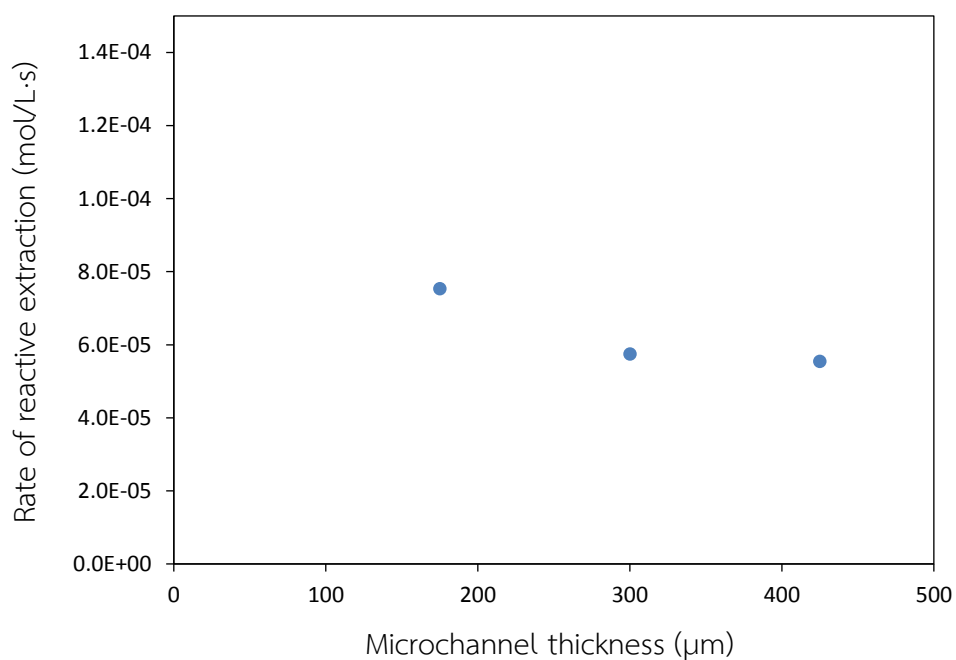


Figure 18 Effect of microchannel thickness on the rate of reactive extraction

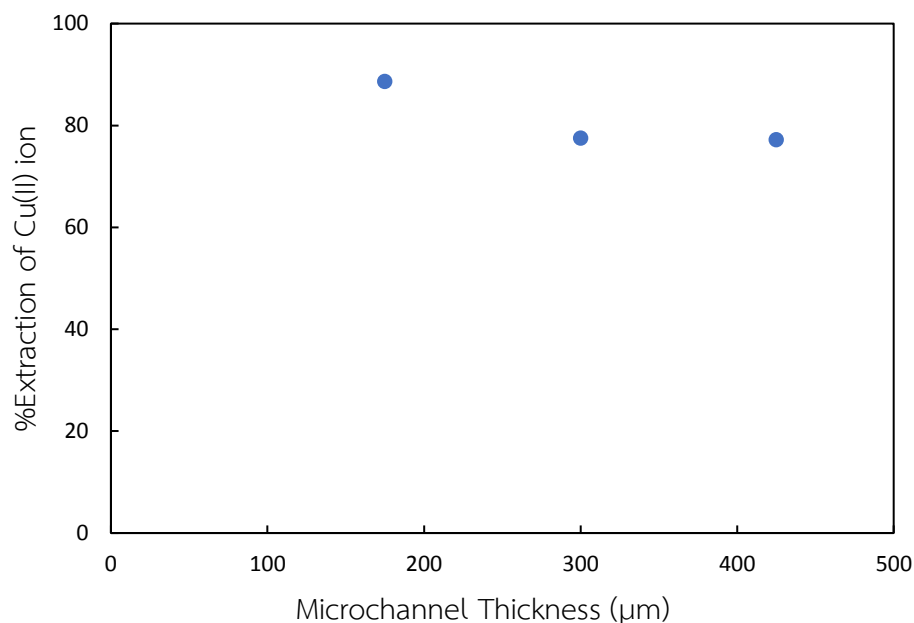


Figure 19 Effect of microchannel thickness on the %extraction of Cu(II) ion

4.2.2 Effect of flow rate on reactive extraction

The effect of flow rate on reactive extraction of metal ion was studied to estimate the rate constant of reactive extraction. Three different flow rates of both solution on each side i.e. 12, 18 and 27 mL under 300 μm of microchannel thickness. Thus, the mean residence time in the microchannel decreases to 200, 133, and 89 sec respectively. Experiment was conducted at a constant initial Cu(II) ion concentration of 1 g/L with a solution of D2EHPA in kerosene (1:1, v/v). The pattern of feeding the solution was the same as 4.2.1. Table 6 shows the concentration of Cu(II) ion at different flow rate. As expected, the concentration of Cu(II) ion at steady state in feed phase decreased with increasing residence time or decreasing the flow rate of solution because the CuSO₄ solution exposed to the extractant in membrane phase for long period of time resulting in more extraction of Cu(II) ion. From the fact that the higher flow rate of the solution leads to a thinner aqueous boundary layer which can reduce the mass transfer resistance and consequently increases the mass

transfer coefficient resulting in higher mass transfer flux across membrane [2]. However, this process occurs within microchannel which can neglect mass transfer resistance as described in 4.2.1. Therefore, increasing the flow rate does not improve the reactive extraction efficiency. The reactive extraction efficiency of Cu(II) ion increased from 66% to 83% when the residence time is increased from 89 to 200 sec as shown in figure 20.

Table 6 The outlet concentration of Cu(II) ion at steady state with different flow rate

Flow rate (mL/hr)	Concentration of Cu(II) ion in feed phase (mg/L)	Concentration of Cu-D2EHPA in membrane phase (mg/L)
12	180.23	1646.65
18	226.27	1881.80
27	354.92	1249.96

(1) Concentration measures at steady state (2) Initial concentration of Cu(II) ion: 1000 mg/L

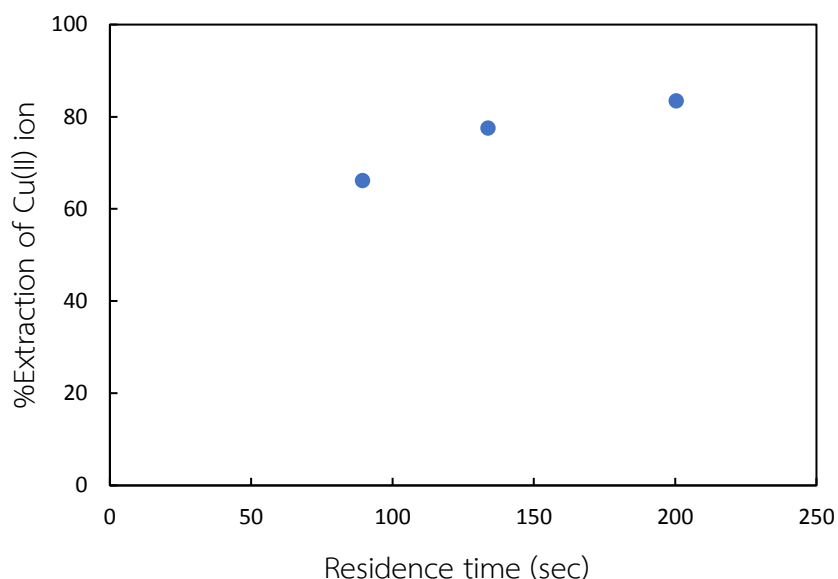


Figure 20 Effect of residence time on the %extraction of Cu(II) ion

The kinetic of the reactive extraction of Cu(II) ion was fitted to the pseudo-second order kinetic model that can be described as equation (5). The rate constant of reactive extraction of Cu(II) ion in microchannel was calculated from the plot of $1/C_t$ versus time with the experiment data at steady state. The relationship of $1/C_t$ versus time was linear which is shown in figure 21 and was confirmed by high value of correlation coefficient $R^2 > 0.95$. The result shows that the rate constant of reactive extraction (k_{ex}) was $5.992 \text{ mol}^{-1}\cdot\text{L}/\text{S}$. The rate of reactive extraction (r_{ex}), as shown in figure 22, was determined according to equation (6), which was 6.46×10^{-5} , 5.75×10^{-5} and $4.00 \times 10^{-5} \text{ mol}/\text{L}\cdot\text{S}$ according to 12, 18 and 27 ml/h of flow rate, respectively.

$$\frac{1}{[C_t]} = k_{ex}t + \frac{1}{[C_0]} \quad (5)$$

$$\text{Rate of reactive extraction } (r_{ex}) = k_{ex} [C_t]^2 \quad (6)$$

Where C_0 , C_t , and t are the initial concentration of Cu(II) ion (mol/L), the concentration of Cu(II) ion at steady state (mol/L) and mean residence time (s)

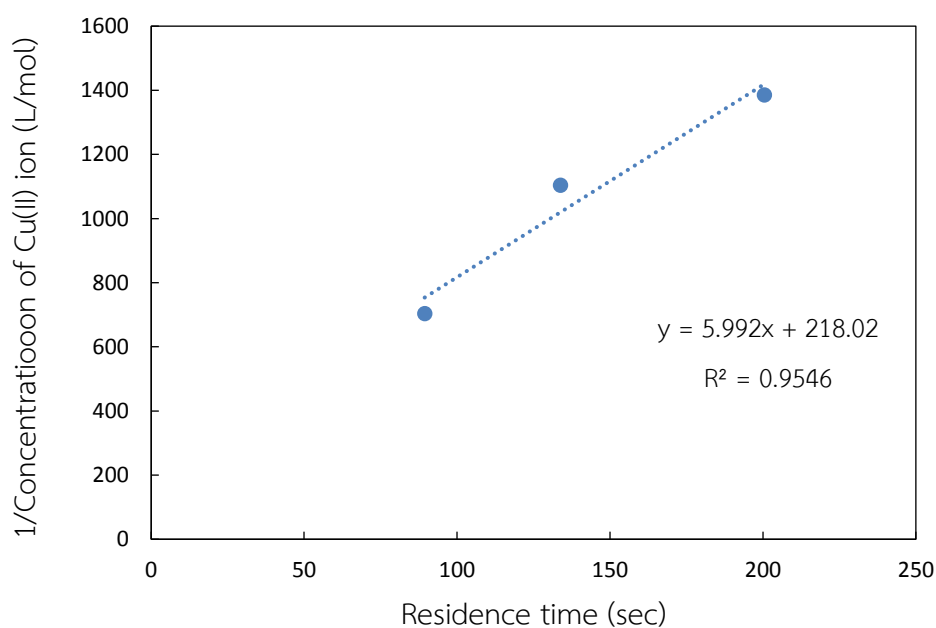


Figure 21 Pseudo-second order kinetic model of reactive extraction of Cu(II) ion

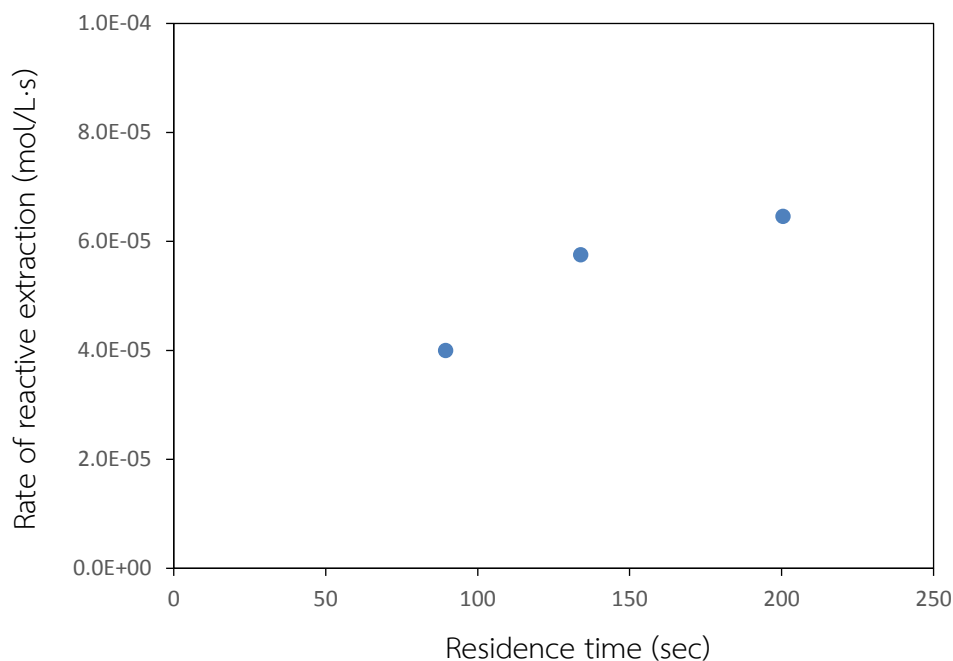


Figure 22 Effect of residence time on the rate of reactive extraction

4.3 The reactive stripping of metal ion

In this part, only reactive stripping is considered. Hence, the system investigated was a microchannel consisting of 2 phases: membrane phase and stripping phase. One side of microchannel was fed with a Cu-D2EHPA complex solution and the other side was fed with HCl solution. In term of Cu-D2EHPA complex solution, it was prepared by mixing between CuSO_4 solution and D2EHPA/kerosene solution in separatory funnel then Cu(II) ions were extracted and transferred to D2EHPA/kerosene solution. The Cu(II) ion in D2EHPA/kerosene solution was used to conduct the experiment. As mention previously, the extraction step occurs at the interface between the feed and membrane phase which requires a stripping step of metal ion at the opposite side of the membrane to achieve overall of the transport process. In the stripping stage, the extractant (D2EHPA/kerosene) is regenerated when reacts with HCl solution and the Cu(II) ion is transferred to

stripping phase. Then, the fresh membrane phase replaced in nanofiber membrane and continued to react with fresh stripping phase. The reaction mechanism can be described as follows: eq. (2) [24]. The effect of microchannel thickness and flow rate of solution were discussed.



where CuR_2 represents Cu-D2EHPA complex solution. H_2R_2 represents D2EHPA/kerosene solution, (aq) represents the species in the aqueous phase and (org) represents the species in the liquid membrane phase.

4.3.1 Effect of microchannel thickness on reactive stripping

The influence of microchannel thickness on reactive stripping of metal ion was studied by varying the thickness of teflon on each side to be 175, 300, and 425 μm . To keep the mean residence time constant at 133 sec, the flow rates of the solutions were adjusted to 10, 18, and 23 mL/h, respectively. The experiment was conducted at constant the initial Cu-D2EHPA complex concentration of 1.5656 g/L with a HCl solution of 6 M. The samples of product were periodically taken every 20 minutes to be measured the concentration of Cu(II) ion by UV-vis. Similarly in 4.2.1, Cu(II) ions are both diffusion from stripping/membrane interface to bulk after stripping reaction and convection from inlet to outlet of microchannel, so mass transfer on reactive stripping also depends on microchannel thickness. From table 7, the result shows that the concentration of Cu(II) ion at steady state in both membrane phase and stripping phase was no significant difference. Moreover, the rate of reactive stripping was also no significant difference, which was 1.44×10^{-6} , 9.16×10^{-7} , 9.55×10^{-7} mol/L-s according to 175, 300 and 425 μm of microchannel thickness, respectively, which shown in figure 23. Because the stripping reaction occurred in microchannel, results in small the mass transfer resistance that can be

neglected. The mass transfer of Cu(II) ion across membrane enhance due to higher driving force of Cu-D2EHPA complex concentration between the two phases. Moreover, the effective mixing of solution in microchannel results in high convection of Cu(II) ion and renews the interface between the two phases. Thus, the reactive extraction system in microchannel overcome mass transfer limitations that play an important role on the rate of reaction. The data of Cu(II) ion concentration at steady state was determined the stripping efficient according to equation (4) which is shown in figure 24. The results showed that the stripping efficiency was slightly different with decreasing the thickness of microchannel, which was 39.39%, 31.34% and 32.00% according to 175, 300 and 425 μm of microchannel thickness. The stripping efficiency of Cu(II) ion does not change significantly as the thickness of microchannel decreased from 425 μm to 175 μm , indicating that the mass transfer of Cu(II) ion from stripping/membrane interface to bulk of membrane phase is not the rate determining step in the reactive stripping process.

Table 7 The outlet concentration of Cu(II) ion at different microchannel thickness on the reactive stripping

Thickness of microchannel (μm)	Concentration of Cu(II) ion in membrane phase (mg/L)	Concentration of Cu(II) ion in stripping phase (mg/L)
175	948.80	123.66
300	1074.86	107.05
425	1064.50	83.64

(1) Concentration measures at steady state (2) Initial concentration of Cu-D2EHPA complex: 1.5656 mg/L

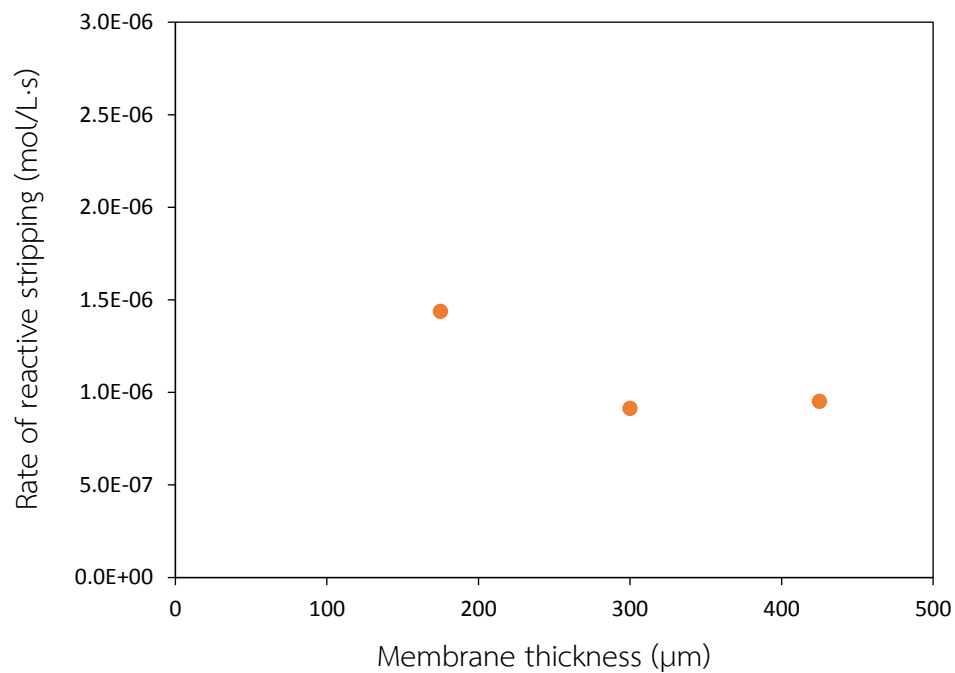


Figure 23 Effect of microchannel thickness on the rate of reactive stripping

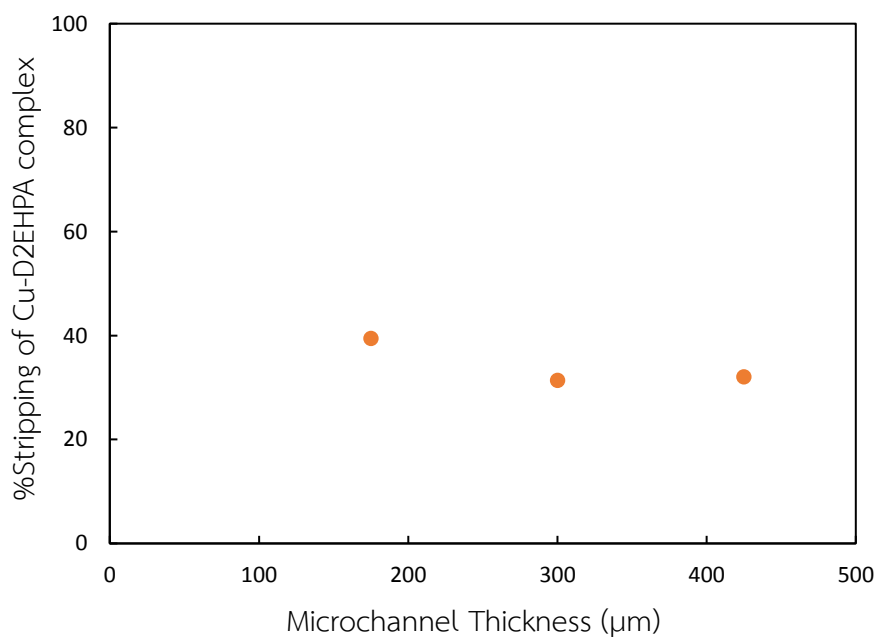


Figure 24 Effect of microchannel thickness on the %stripping of Cu(II) ion

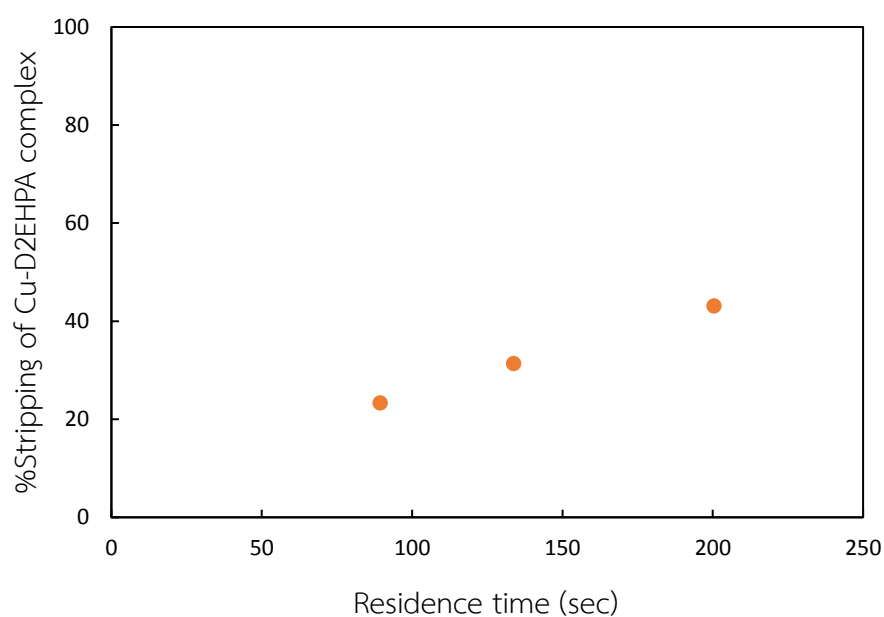
4.3.2 Effect of flow rate on reactive stripping

The effect of flow rate on reactive stripping of metal ions was studied to estimate the rate constant of reactive extraction. Three different flow rates of both solution on each side i.e. 12, 18 and 27 mL/ under 300 μm of microchannel thickness. Thus, the mean residence time in the microchannel decreases to 200, 133, and 89 sec respectively. For all experiment, the initial concentration of Cu-D2EHPA complex solution was conducted at 1.5656 g/L with a 6 M of HCl solution. The pattern of feeding the solution was the same as 4.3.1. Table 8 shows the concentration of Cu(II) ion at steady state with different flow rate on reactive stripping. The results show that the Cu(II) ion was more stripped from Cu-D2EHPA complex in membrane phase when increasing residence time or decreasing the flow rate of solution. This indicated that lower flow rate provided better reactive stripping because of extended contact time which allows molecular diffusion and reaction for longer period of time [41]. Moreover, it is commonly known that the system in microchannel provides $Re < 1$ [42] which can be determined Re as 0.4746 in this study. It indicated that low mixing efficiency and fully dependent on molecular diffusion which is indeed higher flow rate for thinner aqueous boundary layer and lower the mass transfer resistance led to enhance reaction efficiency [43]. However, this process occurs within microchannel which can neglect mass transfer resistance as described in 4.3.1. Therefore, increasing the flow rate does not improve the reactive stripping efficiency. The reactive stripping efficiency of Cu(II) ion increased from 23% to 43% when the residence time is increased from 89 to 200 s, as shown in figure 25.

Table 8 The outlet concentration of Cu(II) ion at steady state with different flow rate

Flow rate (ml/hr)	Concentration of Cu-D2EHPA in outlet of membrane phase (g/L)	Concentration of Cu(II) ion in outlet of stripping phase (g/L)
12	0.89	0.15
18	1.07	0.11
27	1.20	0.08

(1) Concentration measures at steady state (2) Initial concentration of Cu-D2EHPA complex: 1.5656 g/L

**Figure 25** Effect of residence time on the %stripping of Cu-D2EHPA complex

The kinetic of the reactive stripping of Cu(II) ion was fitted to the pseudo-second order kinetic model that can be described as equation (7). The rate constant of reactive stripping of Cu(II) ion in microchannel was calculated from the plot of $1/C_t$ versus time with the experiment data at steady state. The relationship of $1/C_t$ versus time was linear which is shown in figure 26 and is confirmed by high value of

correlation coefficient $R^2 > 0.99$. The results show that the rate constant of reactive stripping is $1.8642 \text{ mol}^{-1}\cdot\text{L}/\text{S}$. The rate of reactive stripping was determined according to equation (8), which was 1.73×10^{-6} , 9.16×10^{-7} , $5.10 \times 10^{-7} \text{ mol}/\text{L}\cdot\text{S}$ according to 10, 18 and 27 mL/h of flow rate, respectively, which shown in figure 27.

$$\frac{1}{[C]_t} = k_{st}t + \frac{1}{[C]_0} \quad (7)$$

$$\text{Rate of reactive stripping } (r_{st}) = k_{st} [C_t]^2 \quad (8)$$

Where C_0 , C_t , k , and t are the initial concentration of Cu-D2EHPA complex (mol/L), the concentration of Cu-D2EHPA complex at steady state (mol/L), the rate constant of reactive stripping ($\text{mol}^{-1}\cdot\text{L}/\text{S}$) and mean residence time (s)

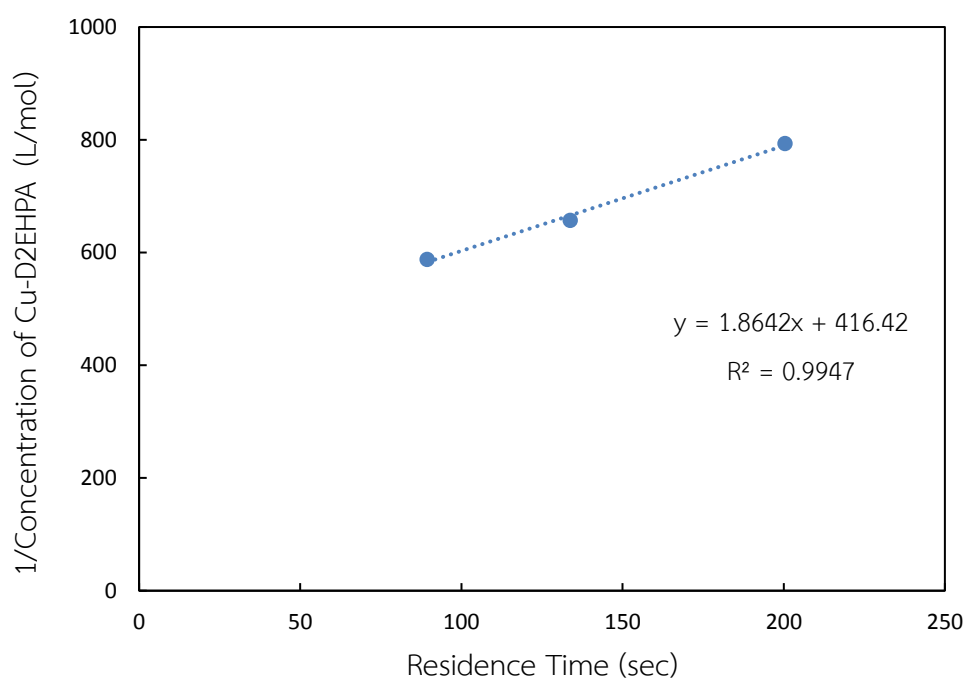


Figure 26 Pseudo-second order kinetic model of reactive stripping of Cu(II) ions

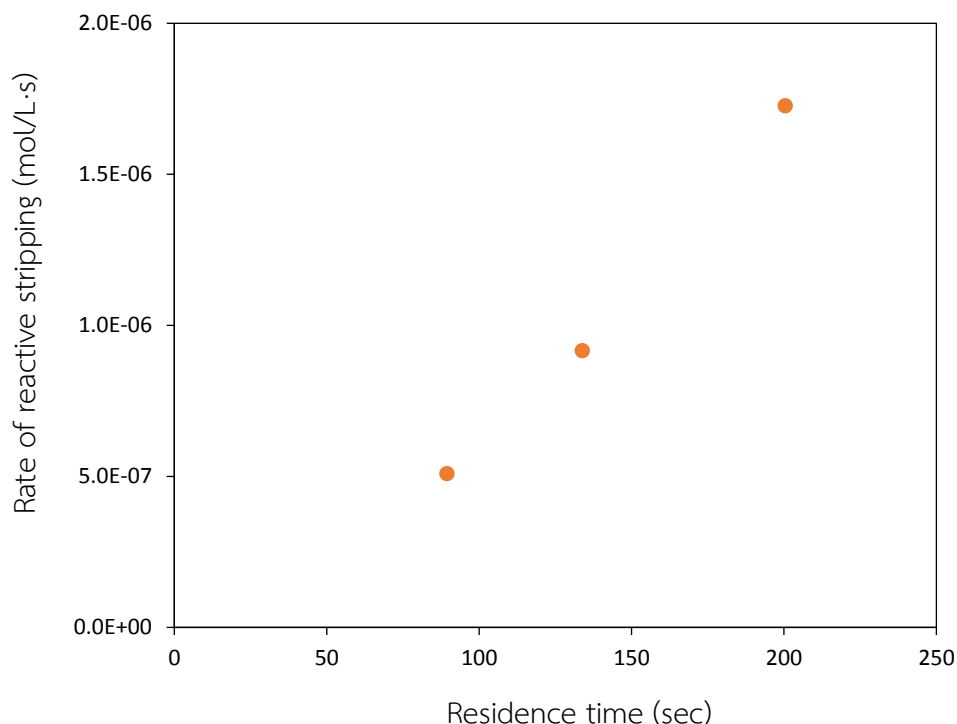


Figure 27 Effect of residence time on the rate of reactive stripping

4.4 Simultaneous reactive extraction and stripping of metal ion

In this part, simultaneous reactive extraction and stripping of metal ion are considered. Hence, the system investigated is a microchannel consisting of 3 phases. The nanofiber membrane of immiscible liquid as membrane phase (D2EHPA/Kerosene) is separated between two miscible liquid as feed phase (CuSO_4 solution) and stripping phase (HCl solution). The Cu(II) ions in feed phase are extracted with extractant at feed/membrane interface as Cu-D2EHPA complex then diffusing across the membrane and are re-extracted to the other side of the membrane into the stripping phase. The reaction mechanism can be described as follows: eq. (1) and (2) [24]. In this process, the transport of Cu(II) ions through liquid membrane consists of 5 step: (i) diffusion of Cu(II) ions from bulk to feed/membrane interface, (ii) the reactive extraction of Cu(II) ions, (iii) diffusion of Cu-D2EHPA

complexes across membrane, (iv) the reactive stripping of Cu-D2EHPA complexes and (v) diffusion of Cu(II) ions from stripping/membrane interface to bulk. The purpose of this work is to identify which step is the rate determining in the process. The effect of nanofiber membrane thickness, initial Cu(II) ion concentration in the feed phase, microchannel thickness, and flow rate of both solution were discussed.

4.4.1 Effect of membrane thickness

The influence of membrane thickness on reactive extraction of metal ions and simultaneous stripping was studied by varying thickness of membrane consisting 361, 497, 830 μm . As for thick membrane, the membrane was prepared by increasing the duration of electrospinning time from 2 hours to 3 and 4 hours, respectively, resulting in more fiber. Thus, the membrane can retain more extractant, but the surface area remains the same. For all experiment, the initial concentration of Cu(II) ion was 1 g/L and the thickness of microchannel was equal to 300 μm . One side of microchannel was fed with a CuSO_4 solution and the other side was fed counter-current with HCl solution under 18 ml/h of flow rate. From table 9, the results show that the concentration of Cu(II) ion is not significantly different between using thin membrane or thick membrane. Although the membrane is thicker and can impregnate a lot of extractant, but the reaction occurs at the interface of membrane which has the same surface area of reaction. Therefore, increasing the thickness does not result in increased efficiency, as shown in figure 28. In addition, the thickness of the membrane in this range is not an obstacle for diffusion of Cu-D2EHPA complexes across the membrane. Thus, the step of Cu-D2EHPA complexes diffusion across membrane is not the rate determining step of this process.

Table 9 The outlet concentration of Cu(II) ion with different thickness of membrane on reactive extraction and stripping

Thickness of membrane (μm)	Conc. of Cu(II) ion in feed phase (g/L)	Conc. of Cu(II) ion in stripping phase (g/L)
361.13	0.60	0.11
497.48	0.67	0.09
829.87	0.61	0.10

Concentration measures at steady state

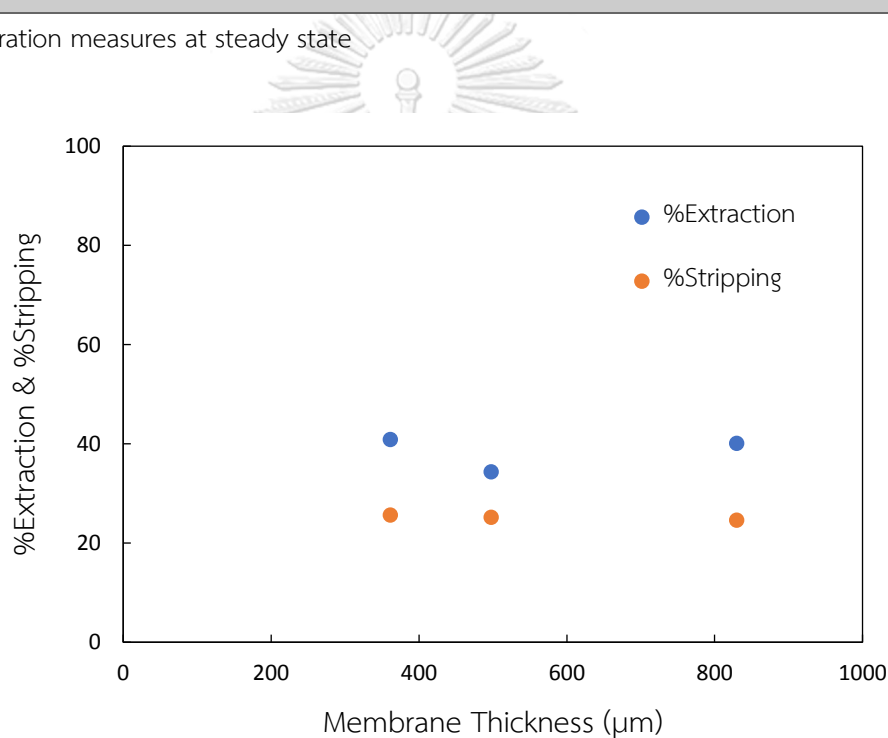


Figure 28 Effect of membrane thickness on simultaneous reactive extraction and stripping

In the simultaneous reactive extraction and stripping process, the transport of Cu(II) ions through liquid membrane consists of 5 steps. To specify which step is rate determining step, the experimental was conducted by considering each reaction, i.e. reactive extraction and reactive stripping as the topic of 4.2 and 4.3, respectively. The results show that the effect of the membrane thickness on the extraction and

stripping efficiency does not change significantly when decreased microchannel thickness from 425 μm to 175 μm indicating that the mass transfer from bulk to feed/membrane interface and stripping/membrane interface to bulk were not the rate determining step in the reactive extraction and stripping process which described as 4.2.1 and 4.3.1, respectively. Moreover, the effect of membrane thickness does not affect on reaction efficient, indicated that the diffusion of Cu-D2EHPA complexes across the membrane was also not the rate determining step which described as 4.4.1. Thus, the remaining two steps consisting of reactive extraction and stripping were considered by comparing the rate of reaction. The rate constant of reactive extraction was 5.992 $\text{mol}^{-1}\cdot\text{L}/\text{S}$ which determined the rate of reactive extraction as 6.46×10^{-5} , 5.75×10^{-5} and 4.00×10^{-5} $\text{mol}/\text{L}\cdot\text{S}$ according to 12, 18 and 27 ml/h of flow rate, respectively. The rate constant of reactive stripping was 1.864 $\text{mol}^{-1}\cdot\text{L}/\text{S}$ which determined the rate of reactive stripping as 1.73×10^{-6} , 9.16×10^{-7} , 5.10×10^{-7} $\text{mol}/\text{L}\cdot\text{S}$ according to 12, 18 and 27 ml/h of flow rate, respectively. The results showed that the rate of reactive extraction was higher than the rate of reactive stripping, indicating that the reactive stripping step was the rate determining step.

4.4.2 Effect of initial Cu(II) concentration in the feed phase

In order to achieve effective removal or recovery of metal ion in microchannel, it is necessary to explore the effect of the initial Cu(II) ion concentration in feed phase on %extraction and %stripping by varying in the range of 0.5-10 g/L with D2EHPA as carrier. For all experiment, the thickness of microchannel was conducted at 250 μm with 6 M of HCl as stripping solution. The flow of the feed and the stripping solution was the counter-current under 18 ml/h of flow rate. The counter-current exchange can achieve a greater amount of mass transfer than co-current because counter-current maintains a slowly declining difference or gradient

concentration [44]. Table 10 shows the concentration of Cu(II) ion at steady state with different initial concentration of Cu(II) ion. The result showed that the concentration of Cu(II) ion decreased rapidly within 20 minutes before the reaction reached steady state, as shown in figure 29. The extraction efficiency increased with decreasing initial Cu(II) ion concentration from 15% to 65%, as shown in figure 30. The higher initial concentration of Cu(II) ion in the feed solution is, the higher the reactive extraction rate at interface of membrane becomes [22]. However, the saturation of membrane pores with Cu-D2EHPA complex results in lower effective membrane area.[29] Therefore, the transport was limited by the diffusion of Cu-D2EHPA complexes through the membrane phase resulting in low efficiency. As for low initial concentration of Cu(II) ion, previous study indicated that the permeation process was controlled by diffusion of Cu(II) ion [29]. However, this problem does not occurred in this study which confirmed that using microchannel overcome the limited by mass transport diffusion of Cu(II) ion, hence the efficient of reaction was still higher. Similarly, the stripping efficiency increased with decreasing initial Cu(II) ion concentration from 18% to 33% in the range of 1-5 g/L. The higher initial concentration of Cu(II) ion resulted in higher Cu-D2EHPA complex. If the metal complex was not completely stripped, the amount of membrane phase in the system decreased and the stripping rate decreased.

Table 10 The outlet concentration of Cu(II) ion with different initial concentration on reactive extraction and stripping

Initial concentration of Cu(II) ion in feed (g/L)	Concentration of Cu(II) ion in feed phase (g/L)	Concentration of Cu(II) ion in stripping phase (g/L)
10	8.43	0.40
5	3.70	0.23
1	0.56	0.12
0.5	0.17	0.11

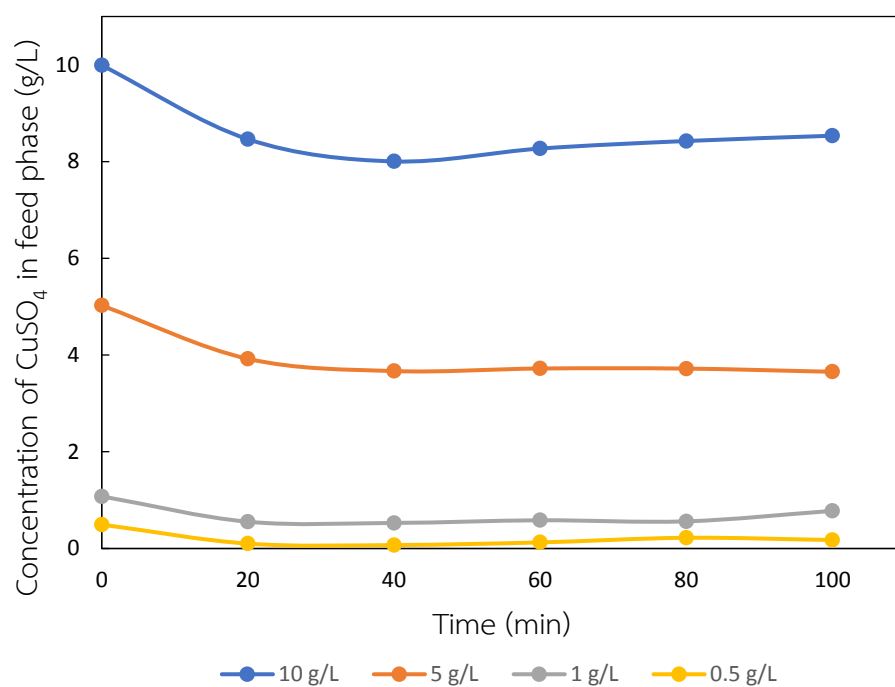


Figure 29 Concentration of CuSO₄ at any time in feed phase

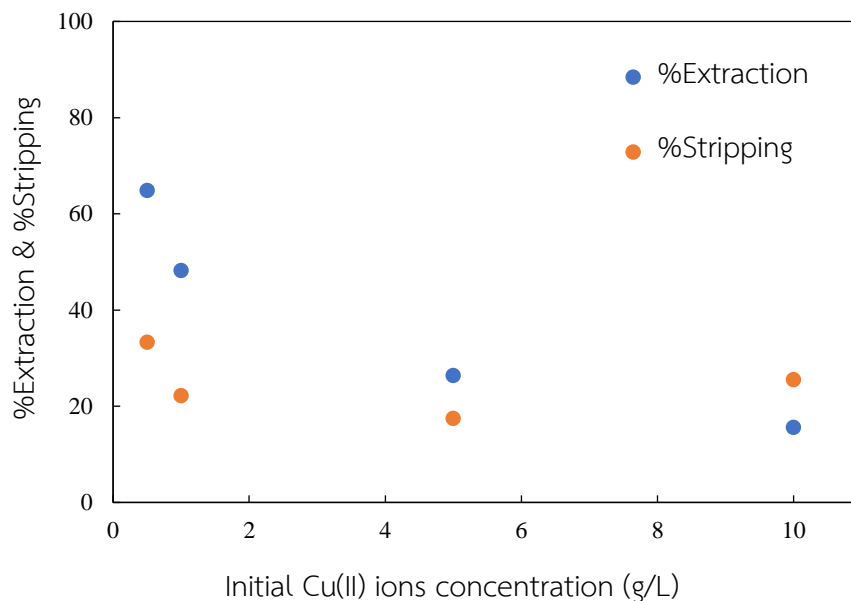


Figure 30 Effect of initial concentration of Cu(II) ion in the feed phase on simultaneous reactive extraction and stripping

4.4.3 Effect of microchannel thickness

The effect of microchannel thickness on reactive extraction of metal ions and simultaneous stripping was studied by varying at the thickness of teflon on each side to be 125, 250, and 500 μm . To keep the mean residence time constant at 118 sec, the flow rates of the solutions was adjusted to 9, 18, and 36 mL/h, respectively. Although the thickness and flow rate were changed but linear velocity did not change. The experiment was conducted at constant initial concentration Cu(II) ion of 1 g/L with HCl solution of 6 M. Table 11 shows the concentration of Cu(II) ion at steady state with different thickness of microchannel. The results confirmed that microchannel thickness affected on simultaneous reactive extraction and stripping. In the large channel, diffusion distance for Cu(II) ions from the feed to the membrane is longer than that in the small channel. Hence, the mass transfer in the small channel is more effective, which increases the chance to react with extractant in the membrane to form metal-complex and improves overall performance of the

extraction. This is confirmed by the experimental results which show that the extraction efficiency increases with decreasing microchannel thickness. The extraction efficiency is 81.92%, 48.21%, and 24.12% and the stripping efficiency is 37.79%, 22.21% and 27.39% with the microchannel thickness of 125, 250, and 500 μm , respectively, as shown in figure 31.

Table 11 The outlet concentration of Cu(II) ion with different microchannel thickness on reactive extraction and stripping

Thickness of microchannel (μm)	Concentration of Cu(II) ion in feed phase (g/L)	Concentration of Cu(II) ion in stripping phase (g/L)
125	0.18	0.30
250	0.56	0.12
500	0.78	0.07

(1) Concentration measures at steady state (2) initial concentration of CuSO_4 : 1 g/L

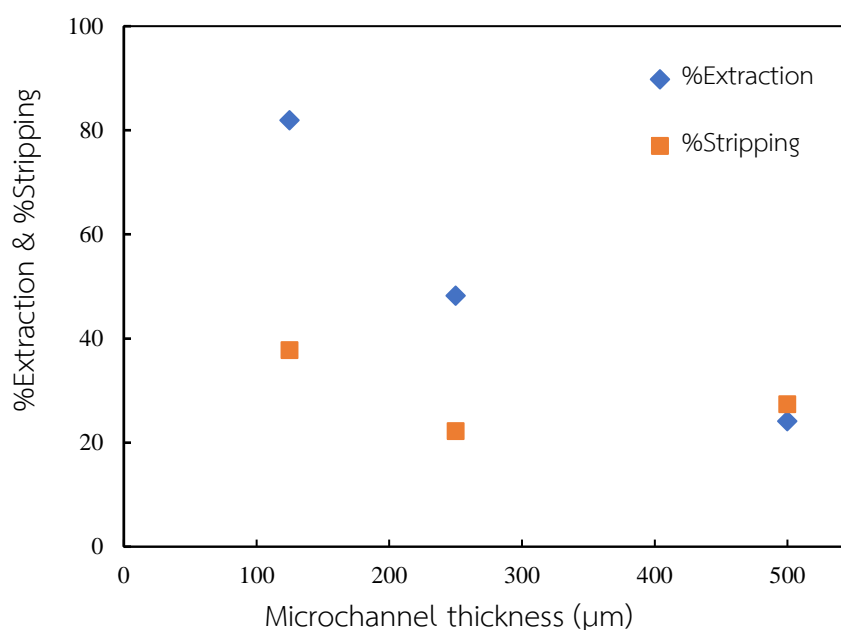


Figure 31 Effect of microchannel thickness on the simultaneous reactive extraction and stripping of Cu(II) ions

4.4.4 Effect of flow rate

The effect of flow rate on reactive extraction and stripping of metal ion were studied. Three different flow rates of both solution on each side were 12, 18 and 27 mL/min under 300 μm of microchannel thickness. Thus, the mean residence time in the microchannel decreased to 200, 133, and 89 sec respectively. Experiments were conducted at a constant initial Cu(II) ion concentration of 1 g/L with a HCl solution of 6 M. Table 12 shows the concentration of Cu(II) ion at different flow rate. As expected, the concentration of Cu(II) ion at steady state in feed phase decreased with increasing residence time or decreasing the flow rate of solution because the CuSO_4 solution exposed to the extractant in membrane phase for longer period of time resulting in more extraction of Cu(II) ion. On the other hand, the concentration of Cu(II) ion in stripping phase increased when increasing residence time due to extended contact time to react with stripping phase. From the fact that the higher flow rate of the solution leads to a thinner aqueous boundary layer which can reduce the mass transfer resistance and consequently increases the mass transfer coefficient resulting in higher mass transfer flux across membrane [2]. However, this process occurs within microchannel which can neglect mass transfer resistance. Therefore, increasing the flow rate does not improve the reactive extraction efficiency. The reactive extraction efficiency of Cu(II) ion increased from 33% to 46% and the reactive stripping efficiency of Cu(II) ion increased from 17% to 32% when the residence time is increased from 89 to 200 sec as shown in figure 32.

Table 12 The outlet concentration of Cu(II) ion with different flow rate on reactive extraction and stripping

Flow rate (ml/hr)	Concentration of Cu(II) ion in feed phase (g/L)	Concentration of Cu(II) ion in stripping phase (g/L)
27	0.69	0.06
18	0.60	0.11
12	0.55	0.15

(1) Concentration measures at steady state (2) initial concentration of CuSO_4 : 1 g/L

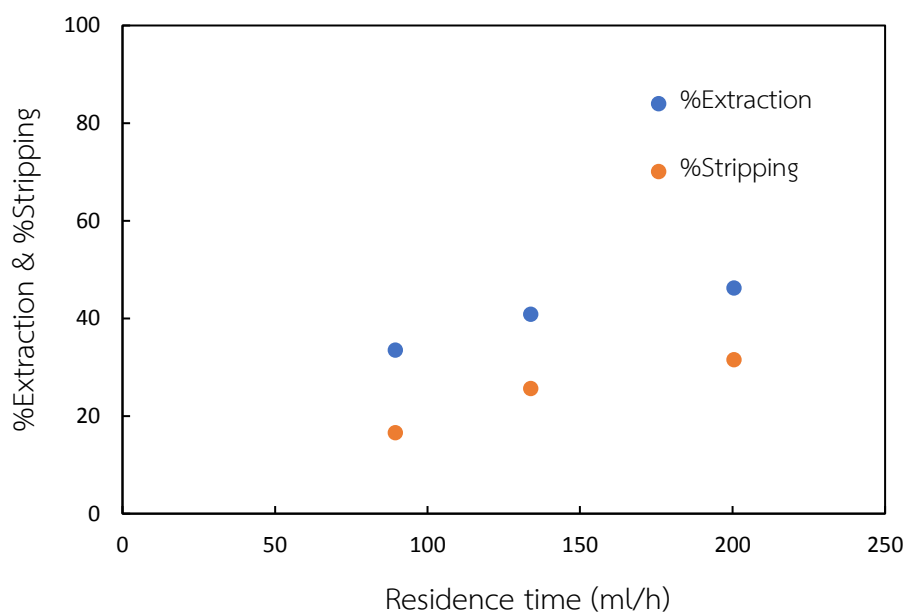


Figure 32 Effect of residence time on the simultaneous reactive extraction and stripping of Cu(II) ions

CHAPTER V

CONCLUSIONS AND RECOMMENDATIONS

5.1 Conclusions

This work intends to recover ions of heavy metal from wastewater using reactive extraction by nanofibers-supported liquid membrane (NSLM) in a microchannel. The PVDF nanofibers membrane were successfully prepared with random interconnected structure by electrospinning with average diameter about 70-170 nm and can effectively support the liquid membrane. The applied NSLM in a microchannel could minimize mass transfer resistance, hence improving overall performance of the reactive extraction. The results show that the diffusion of Cu(II) from bulk to interface of membrane and diffusion of Cu-D2EHPA complexes across the membrane were not the rate determining step. The rate of reactive extraction was higher than the rate of reactive stripping, indicating that the reactive stripping step was the rate determining step. The efficiency of extraction metal ions can be extracted up to 82% at 1 g/L of initial concentration of metal ions, 125 μm of microchannel thickness and 9 ml/h of flow rate.

5.2 Recommendation

1. Change the copper (II) ion in feed phase solution to other metal ion to more understand kinetic control the reactive extraction and stripping in microchannel
2. Studying the effect of concentration of HCl solution to improve the rate of reactive stripping.
3. Using the raw data to validate in computational fluid dynamics (CFD) and to determined flux of reaction, mass transfer coefficient, concentration profile, etc.



APPENDIX A

Calibration Data Analysis

Concentration of Cu(II) ions in both outlet solution from microchannel can determine by ultraviolet-visible spectrophotometer (UV-Vis). The standards of CuSO_4 solution were prepared different concentration in the range of 0.2-1.2 g/L and 5-25 g/L to establish the calibration curve of Cu(II) ions which shows in the figure.

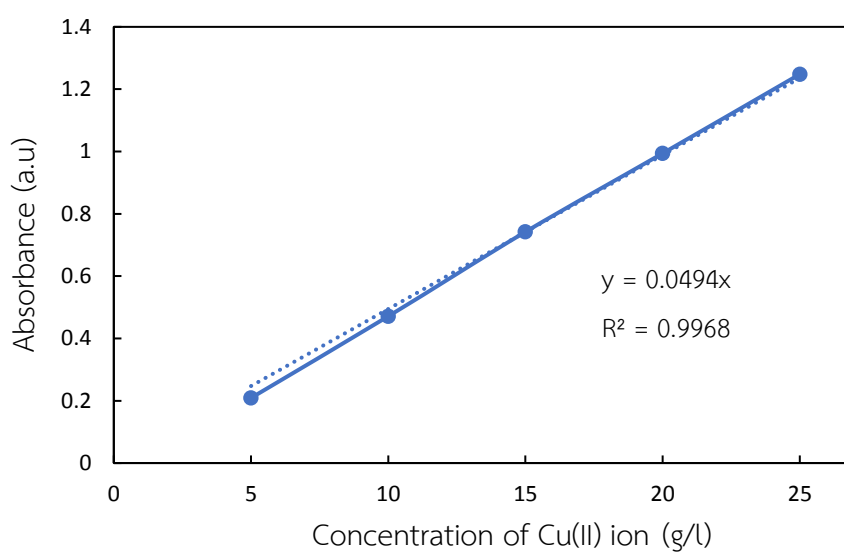


Figure 33 Calibration curve of Cu(II) ion in the range of 5-25 g/L

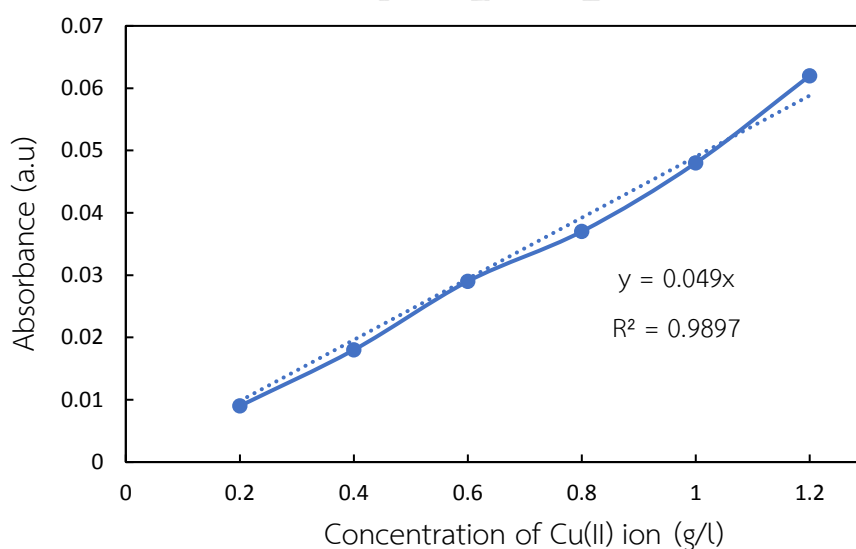


Figure 34 Calibration curve of Cu(II) ion in the range of 0.2-1.2 g/L

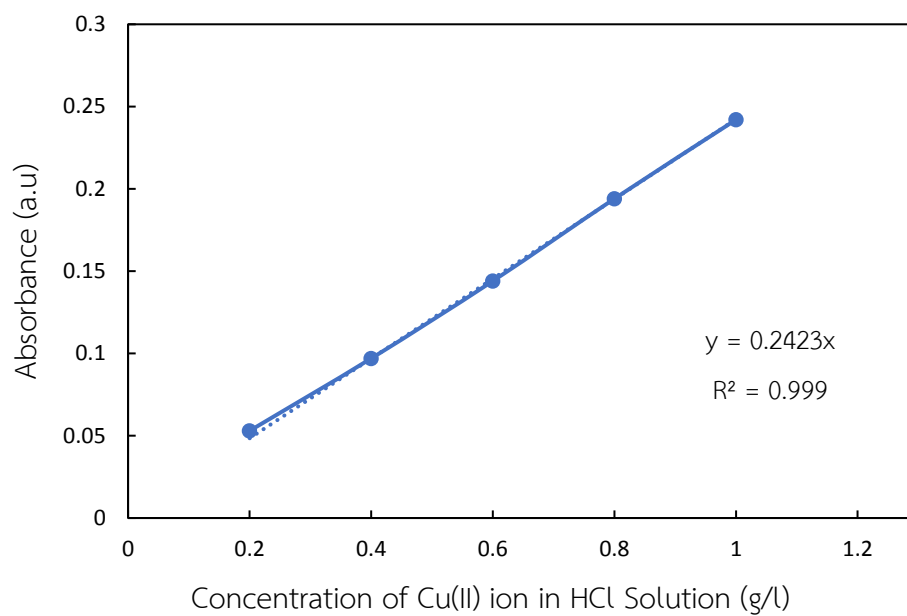


Figure 35 Calibration curve of Cu(II) ion in HCl Solution

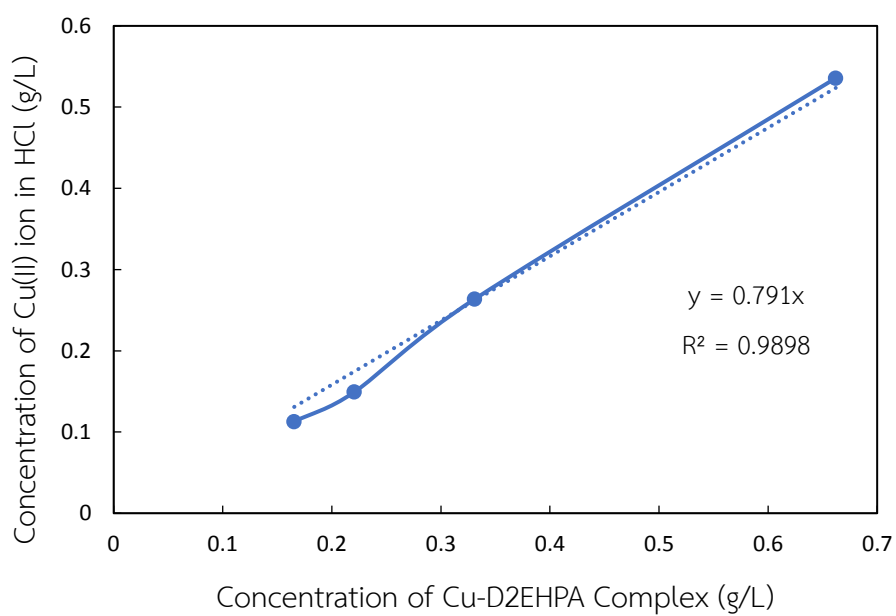


Figure 36 Calibration curve of Cu-D2EHPA complex concentration

APPENDIX B

PROCEDURE OF CHEMICAL PREPARATION

B.1 Preparation of CuSO_4 Solution

- Add 0.05, 0.1, 0.5 and 1 g of CuSO_4 in 100 ml of the volumetric flask for concentration of CuSO_4 at 0.5, 1, 5 and 10 g/L, respectively.
- Then add deionized water to make 100 ml of total volume.

B.2 Preparation of HCl Solution (6 Molar)

- Add 52 ml of HCl (37 %wt) in 100 ml of the volumetric flask.
- Then add deionized water to make 100 ml of total volume.

B.3 Preparation of D2EHPA/Kerosene (1:1 v/v ratio) Solution

- Add 50 ml of D2EHPA in 100 ml of the volumetric flask.
- Then add kerosene to make 100 ml of total volume.

B.4 Preparation of Cu-D2EHPA Complex

- Prepare CuSO_4 solution at 5 g/L, according to B.1, in separatory funnel
- Then add D2EHPA/Kerosene (1:1 v/v ratio) solution from B.3 and shake the mixture solution.

B.4 Preparation of PVDF solution (15 %wt)

- Add 1.5 g of PVDF in 100 ml of beaker.
- Then add N,N-dimethyl formamide (DMF) to make 10 ml of total volume.
- Then stirred for 45 minutes at 60 °C using hot plate until a homogeneous solution was formed.

APPENDIX C

CALCULATION

C.1 Calculation of %extraction and %stripping efficiency

$$EE (\%) = \frac{C_{fo} - C_{ft}}{C_{fo}} \times 100 \quad (3)$$

$$SE (\%) = \frac{C_{st}}{C_{fo} - C_{ft}} \times 100 \quad (4)$$

Where C_{fo} is the initial concentration of Cu(II) in the feed phase and C_{ft} , C_{st} are the concentration in the feed phase and stripping phase at any time.

Example: The data of reactive extraction of copper and simultaneous stripping (1 g/L of CuSO_4 concentration, thickness of 125 μm , flow rate is 9 ml/h)

Time (min)	$[\text{Cu(II)}]_{ft}$ (g/L)	$[\text{Cu(II)}]_{st}$ (g/L)
0	0.982	0
20	0.2269	0.7621
40	0.2025	0.5424
60	0.2244	0.2864
80	0.2212	0.3627
100	0.2211	0.2522
120	0.2175	0.2376
140	0.1763	0.2887
160	0.1787	0.254

- The initial concentration of Cu(II) ion is 0.982 g/L
- The average concentration of Cu(II) ion at steady state in feed phase is 0.1775 g/L

- The average concentration of Cu(II) ion at steady state in stripping phase is 0.2714 g/L

$$\begin{aligned} \text{EE (\%)} &= \frac{0.9820 - 0.1775}{0.9820} \times 100 \\ &= 81.92\% \end{aligned}$$

$$\begin{aligned} \text{SE (\%)} &= \frac{0.2714}{0.9820 - 0.1775} \times 100 \\ &= 33.73\% \end{aligned}$$

C.2 Calculation of residence time (RT)

Residence time is a measure of the time taken for the solution to pass through a microchannel

$$\text{Residence time (RT)} = \frac{\text{Volume of reactor (mL)}}{\text{Flow rate (mL/hr)}}$$

$$= \frac{0.6688 \text{ mL}}{18 \text{ mL/hr}}$$

$$= 0.0372 \text{ hr}$$

$$= 2.23 \text{ min}$$

$$= 133.8 \text{ sec}$$

APPENDIX D

RAW DATA

D.1 The Cu(II) ion concentration data of reactive extraction (2 phase: feed phase and membrane phase) at microchannel thickness in the range of 175-425 μm with 1g/L of initial concentration

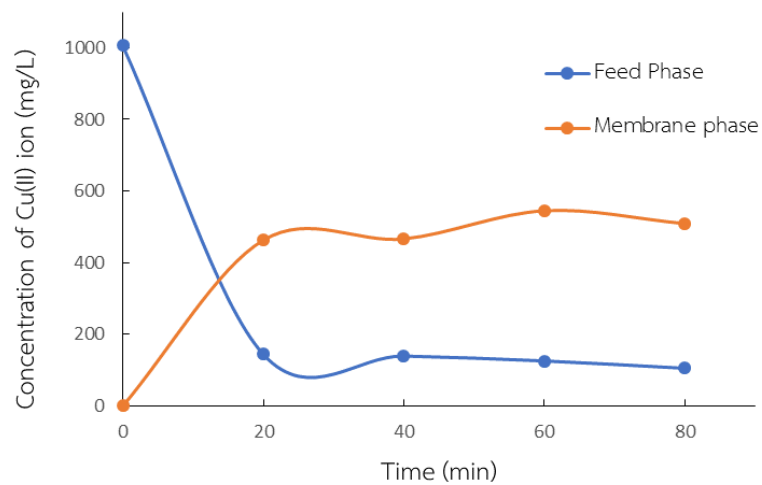


Figure 37 The concentration of Cu(II) ion in the feed phase and membrane phase at any time (thickness = 175 μm)

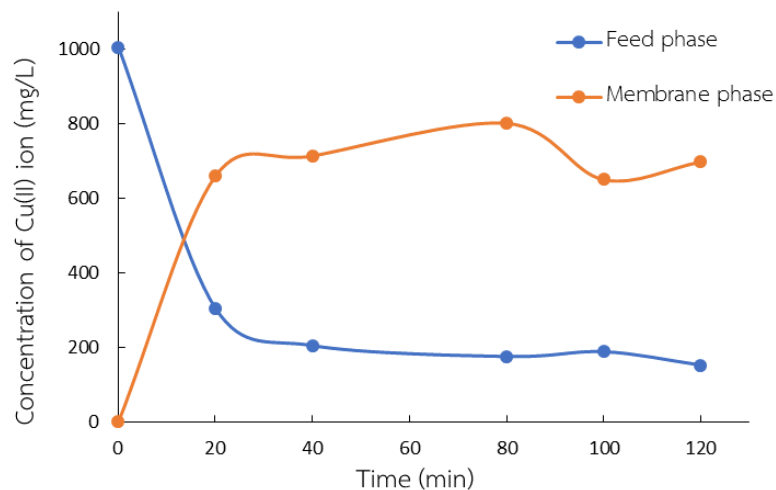


Figure 38 The concentration of Cu(II) ion in the feed phase and stripping phase at any time (thickness = 300 μm)

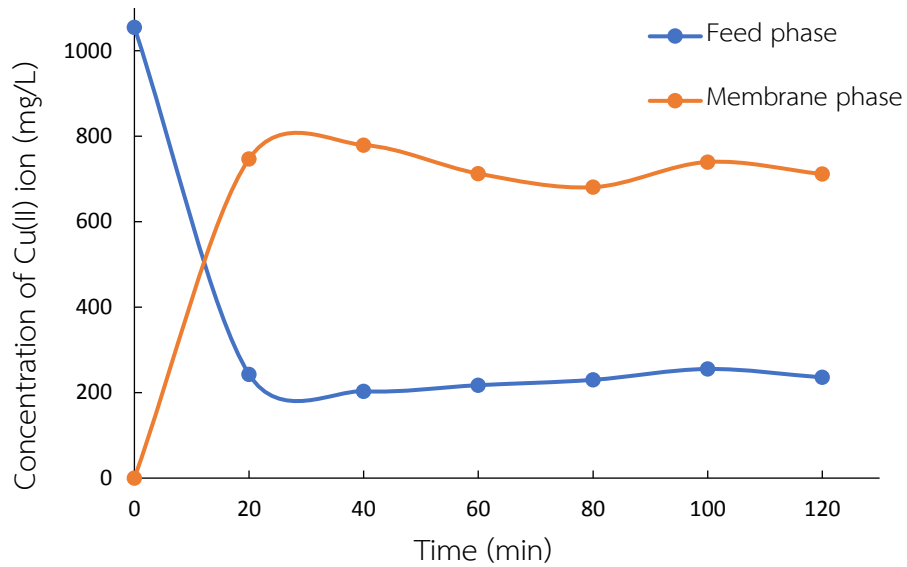


Figure 39 The concentration of Cu(II) ion in the feed phase and stripping phase at any time (thickness = 425 μm)

D.2 The Cu(II) ion concentration data of reactive extraction (2 phase: feed phase and membrane phase) at flow rate of solution in the range of 12-27 ml/h with 300 μm of microchannel thickness and 1 g/L of initial concentration

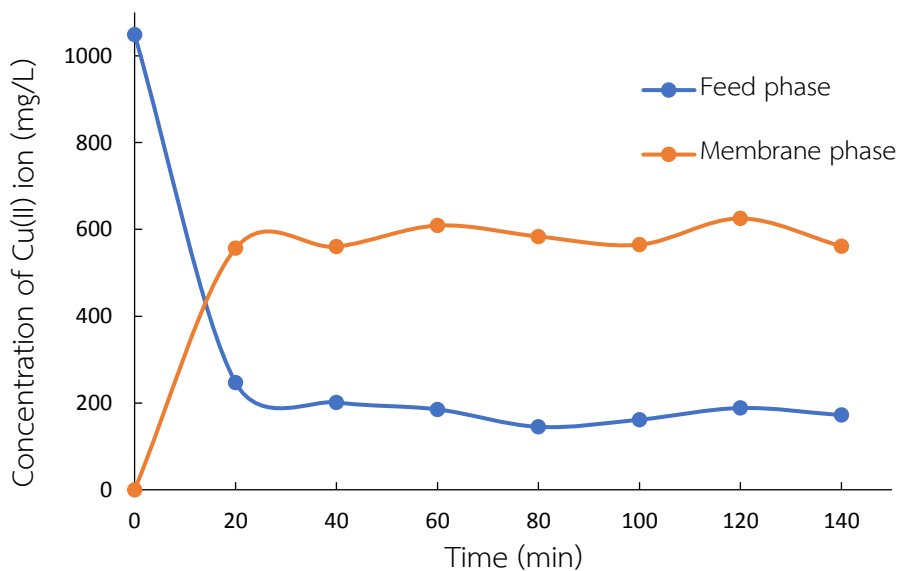


Figure 40 The concentration of Cu(II) ion in the feed phase and membrane phase at any time (Flow rate = 12 ml/h)

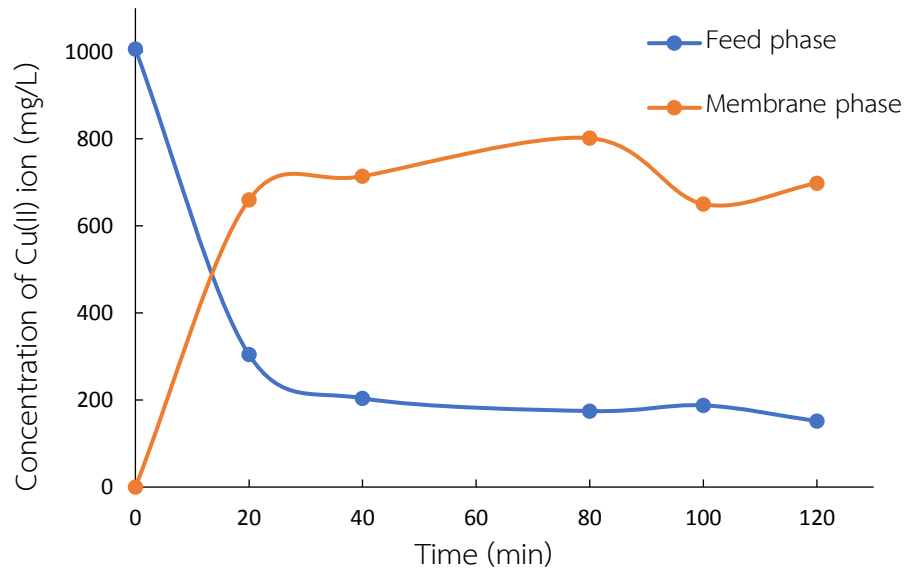


Figure 41 The concentration of Cu(II) ion in the feed phase and membrane phase at any time (Flow rate = 18 ml/h)

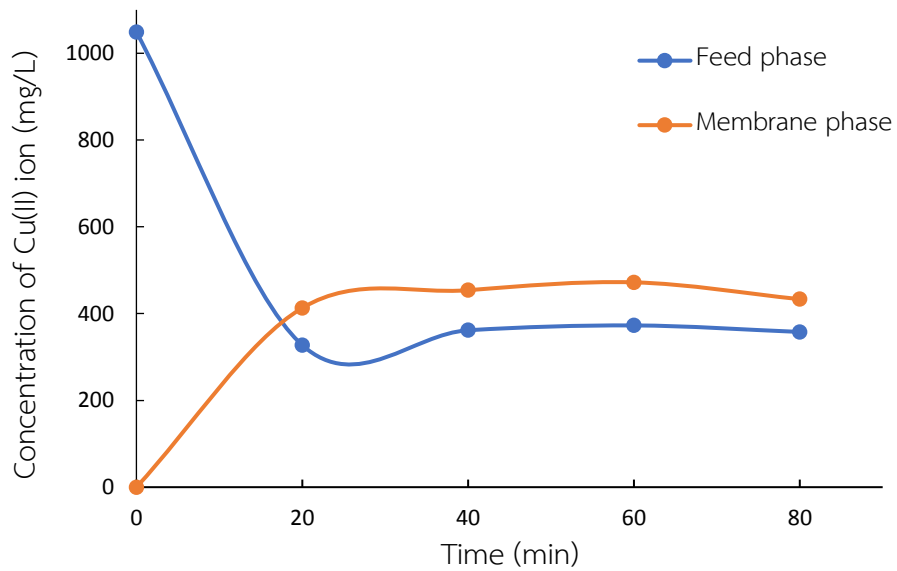


Figure 42 The concentration of Cu(II) ion in the feed phase and membrane phase at any time (Flow rate = 27 ml/h)

D.3 The Cu(II) ion concentration data of reactive stripping (2 phase: membrane phase and stripping phase) at microchannel thickness in the range of 175-425 μm with 1g/L of initial concentration

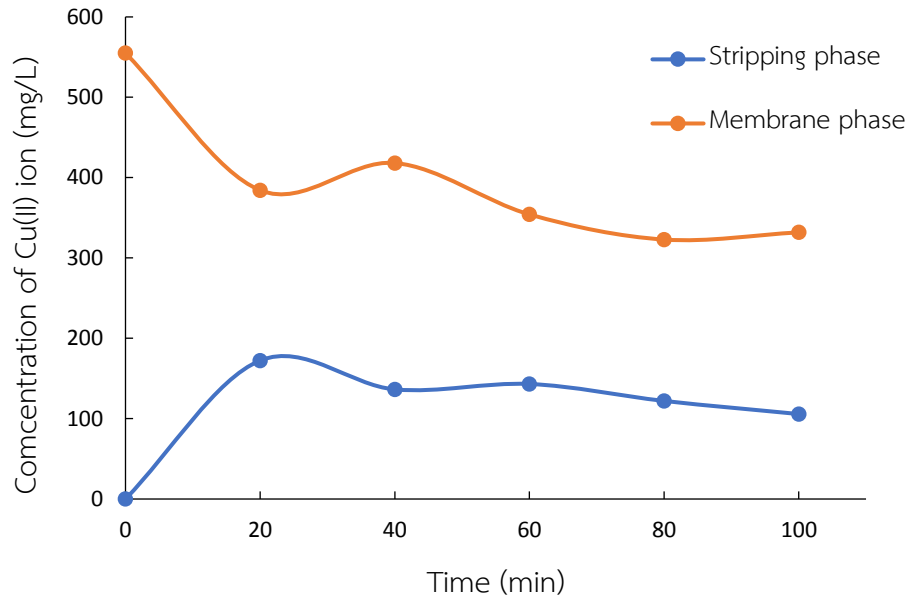


Figure 43 The concentration of Cu(II) ion in the membrane phase and stripping phase at any time (thickness = 175 μm)

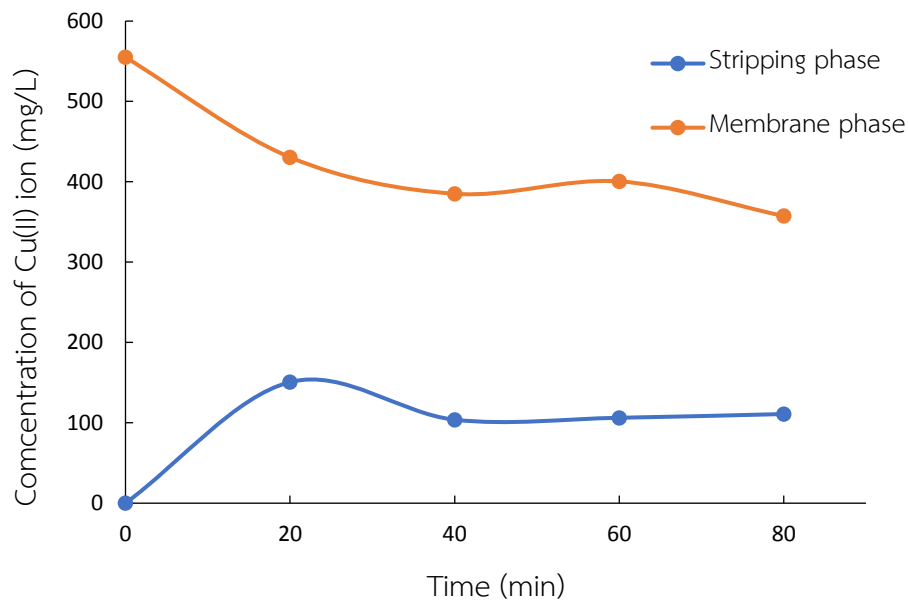


Figure 44 The concentration of Cu(II) ion in the membrane phase and stripping phase at any time (thickness = 300 μm)

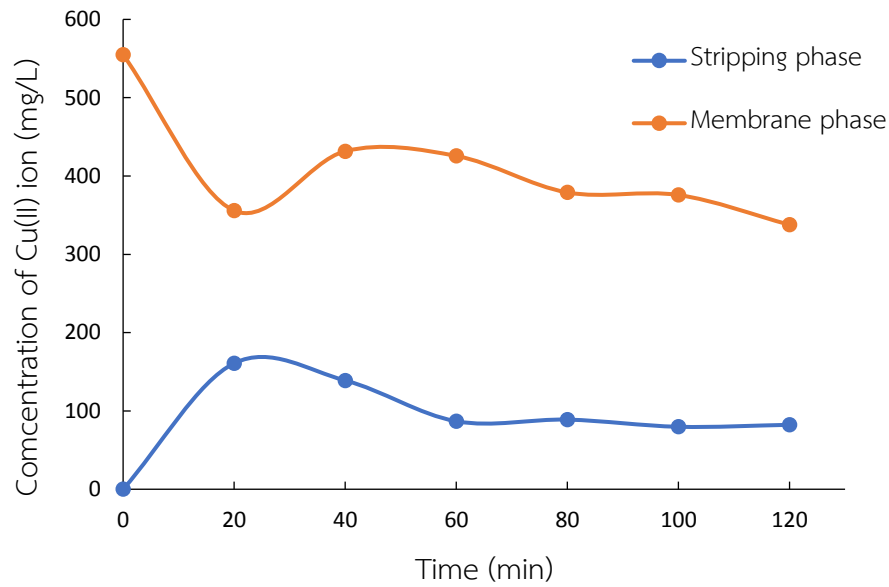


Figure 45 The concentration of Cu(II) ion in the membrane phase and stripping phase at any time (thickness = 425 μm)

D.4 The Cu(II) ion concentration data of reactive stripping (2 phase: membrane phase and stripping phase) at flow rate of solution in the range of 12-27 ml/h with 300 μm of microchannel thickness and 1 g/L of initial concentration

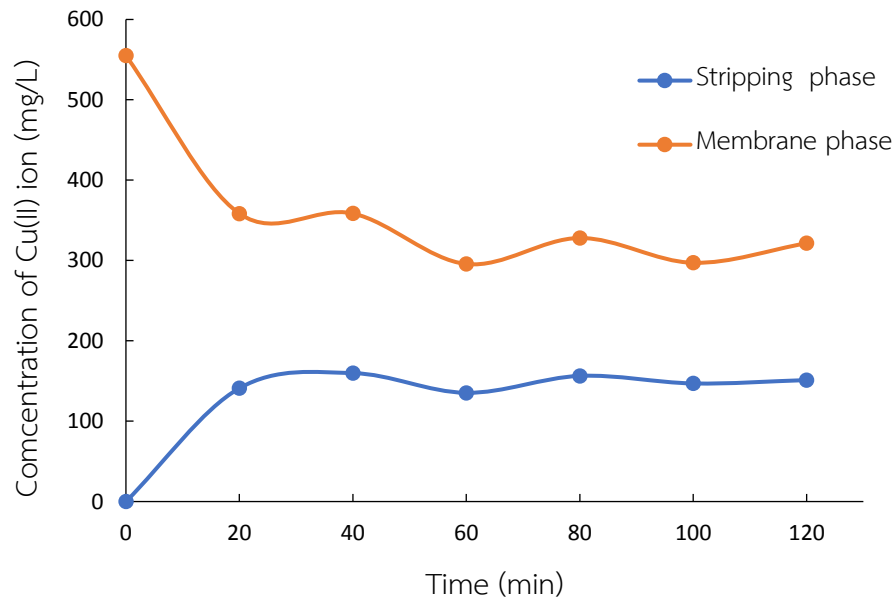


Figure 46 The concentration of Cu(II) ion in the membrane phase and stripping phase at any time (Flow rate = 12 ml/h)

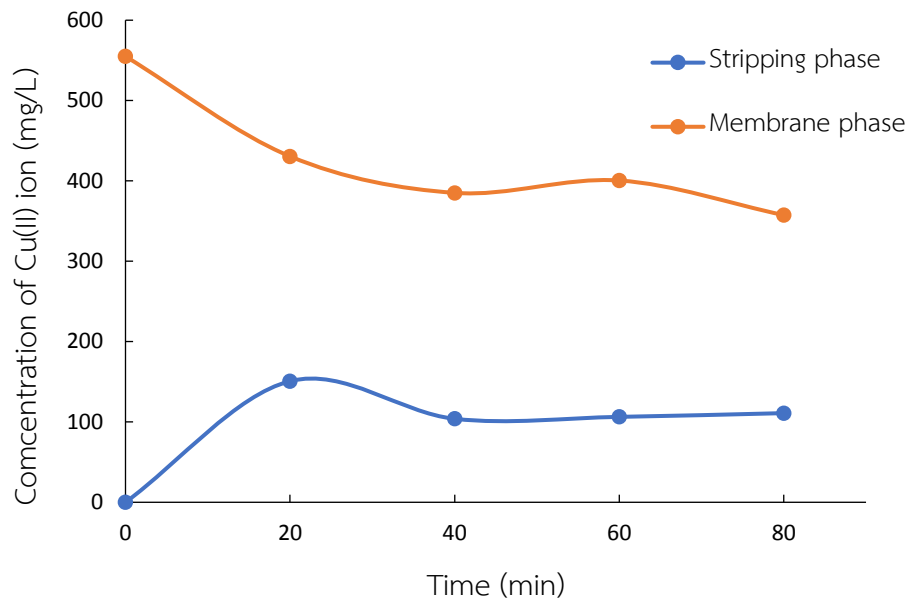


Figure 47 The concentration of Cu(II) ion in the membrane phase and stripping phase at any time (Flow rate = 18 ml/h)

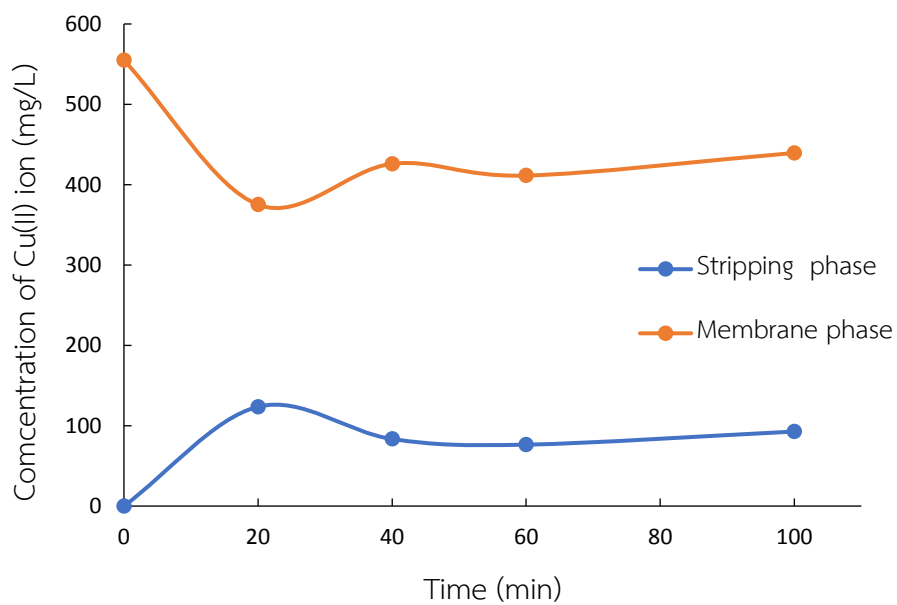


Figure 48 The concentration of Cu(II) ion in the membrane phase and stripping phase at any time (Flow rate = 27 ml/h)

D.5 The Cu(II) ion concentration data of reactive extraction of copper and simultaneous stripping (3 phase) at initial concentration of CuSO_4 in the range of 0.5-10 g/L with 250 μm of microchannel thickness and 18 mL/h of flow rate

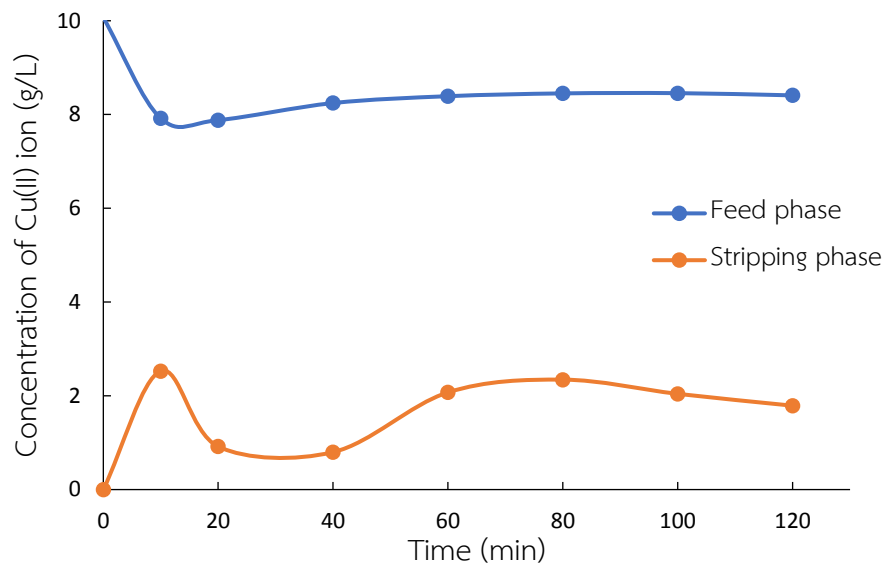


Figure 49 The concentration of Cu(II) ion in the feed phase and stripping phase at any time (initial concentration = 10 g/L)

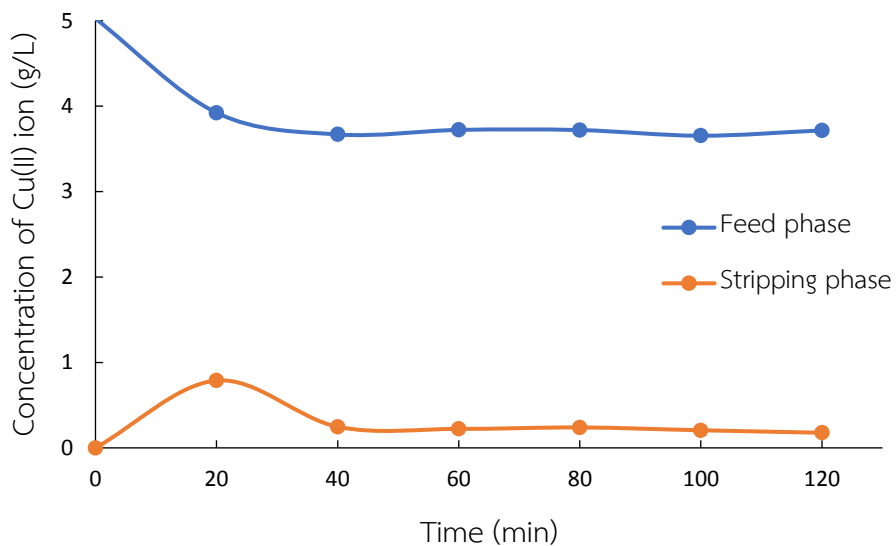


Figure 50 The concentration of Cu(II) ion in the feed phase and stripping phase at any time (initial concentration = 5 g/L)

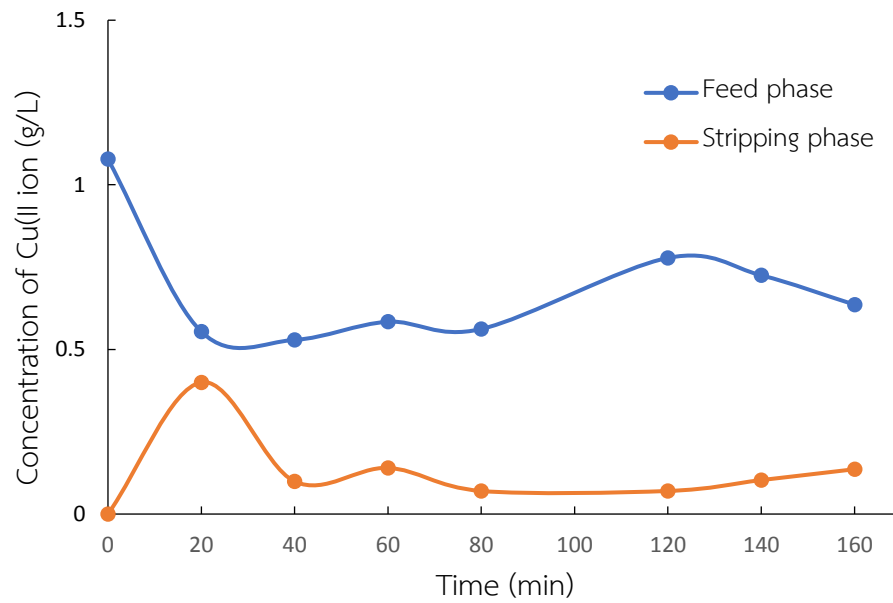


Figure 51 The concentration of Cu(II) ion in the feed phase and stripping phase at any time (initial concentration = 1 g/L)

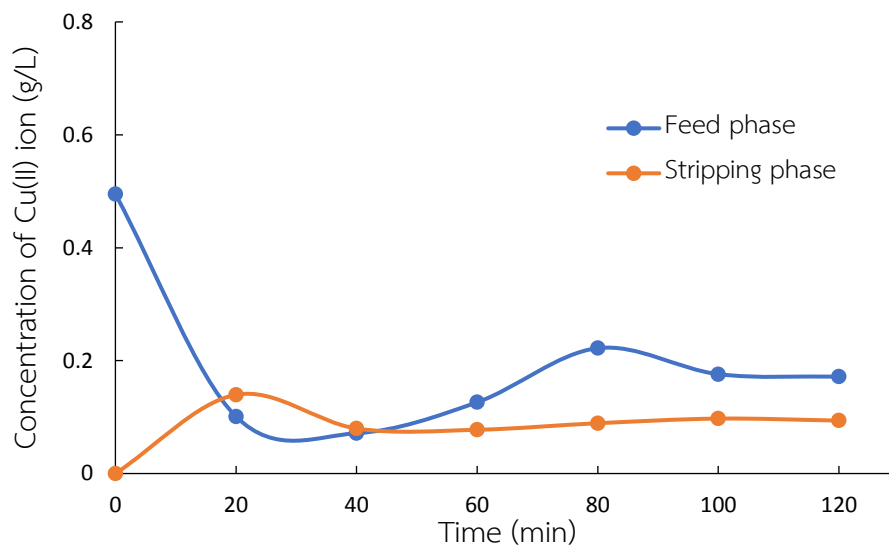


Figure 52 The concentration of Cu(II) ion in the feed phase and stripping phase at any time (initial concentration = 0.5 g/L)

D.6 The Cu(II) ion concentration data of reactive extraction of copper and simultaneous stripping (3 phase) at thickness of microchannel in the range of 125-500 μm with 1 g/L of initial concentration

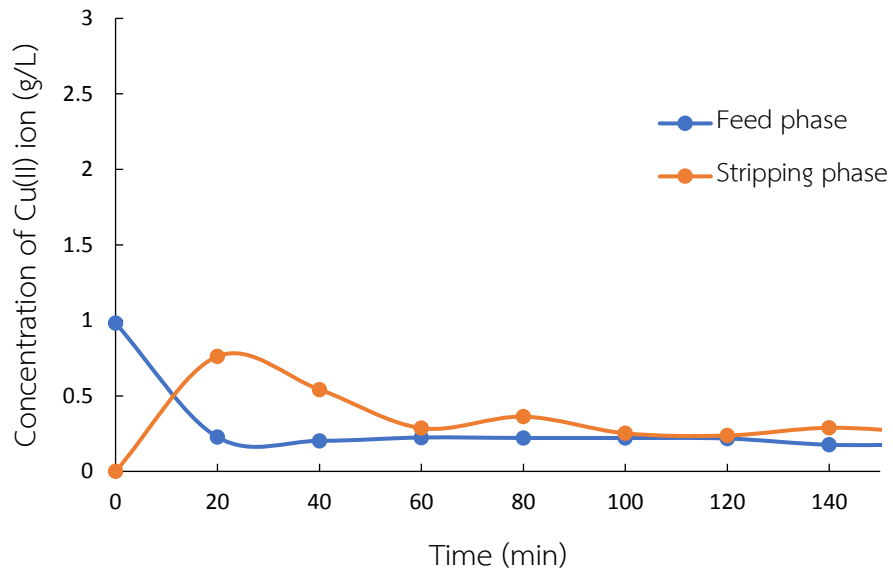


Figure 53 The concentration of Cu(II) ion in the feed phase and stripping phase at any time (thickness = 125 μm)

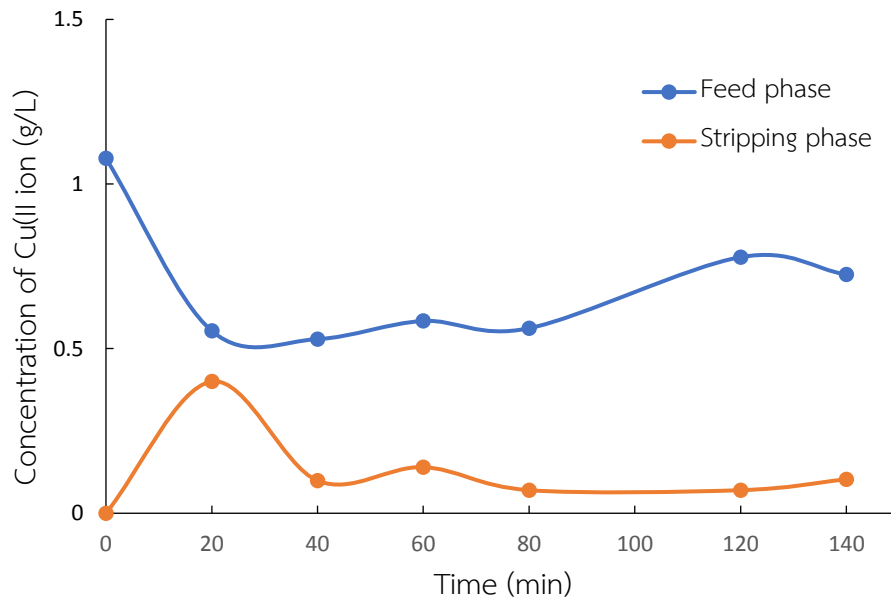


Figure 54 The concentration of Cu(II) ion in the feed phase and stripping phase at any time (thickness = 250 μm)

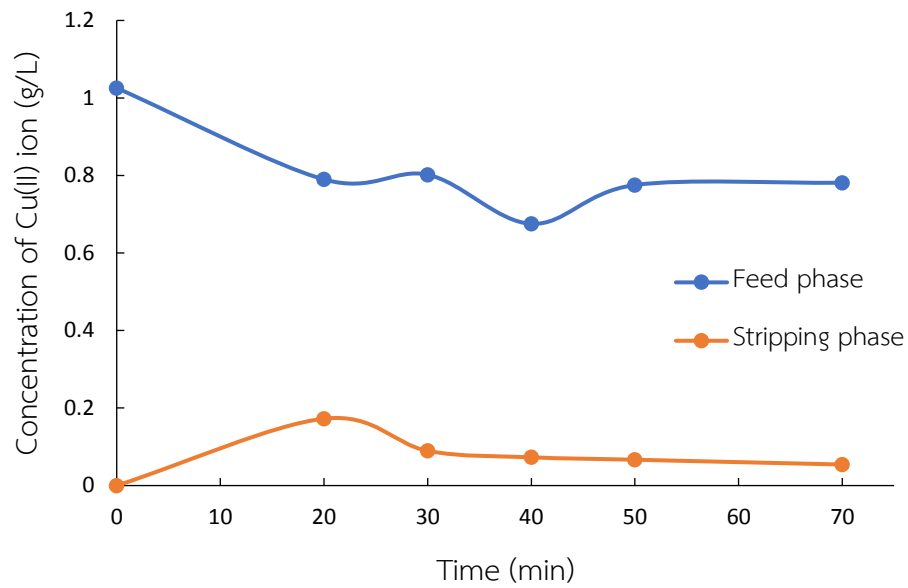


Figure 55 The concentration of Cu(II) ion in the feed phase and stripping phase at any time (thickness = 500 μm)

D.7 The Cu(II) ion concentration data of reactive extraction of copper and simultaneous stripping at flow rate in the range of 12-27 mL/h with 300 μm of microchannel thickness and 1 g/L of initial concentration

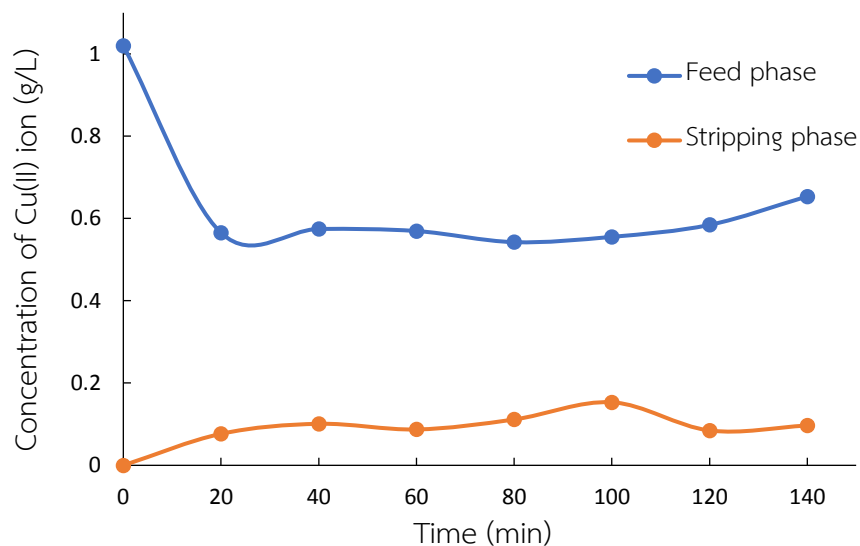


Figure 56 The concentration of Cu(II) ion in the feed phase and stripping phase at any time (Flow rate = 12 mL/h)

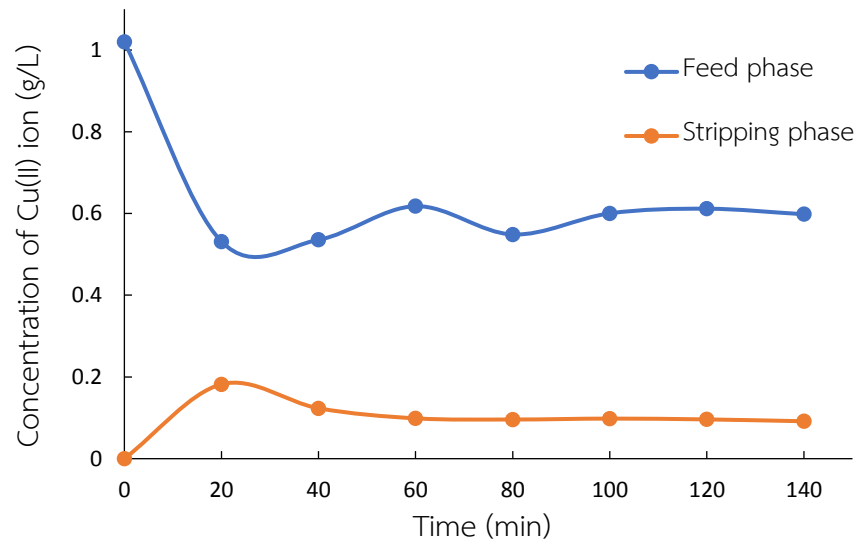


Figure 57 The concentration of Cu(II) ion in the feed phase and stripping phase at any time (Flow rate = 18 ml/h)

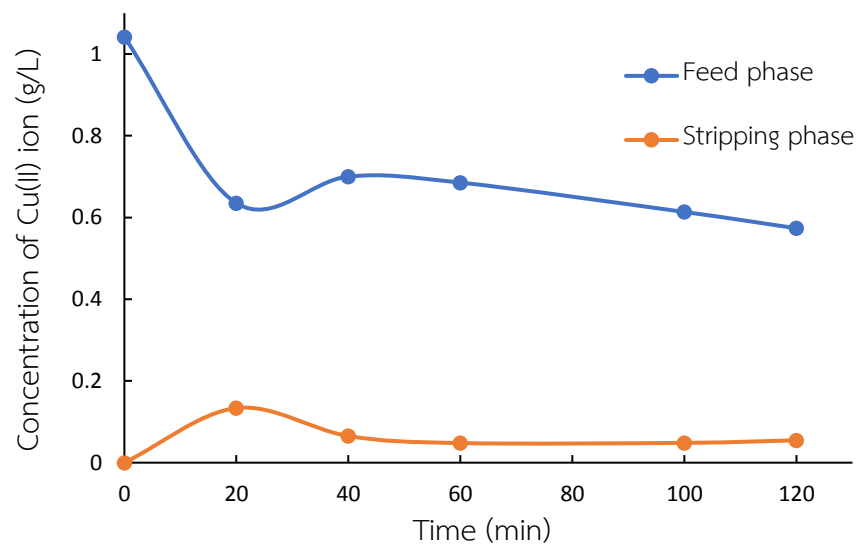


Figure 58 The concentration of Cu(II) ion in the feed phase and stripping phase at any time (Flow rate = 27 ml/h)

D.8 The Cu(II) ion concentration data of reactive extraction of copper and simultaneous stripping (3 phase) at different membrane thickness with 10 g/L of initial concentration and 300 μm of microchannel thickness

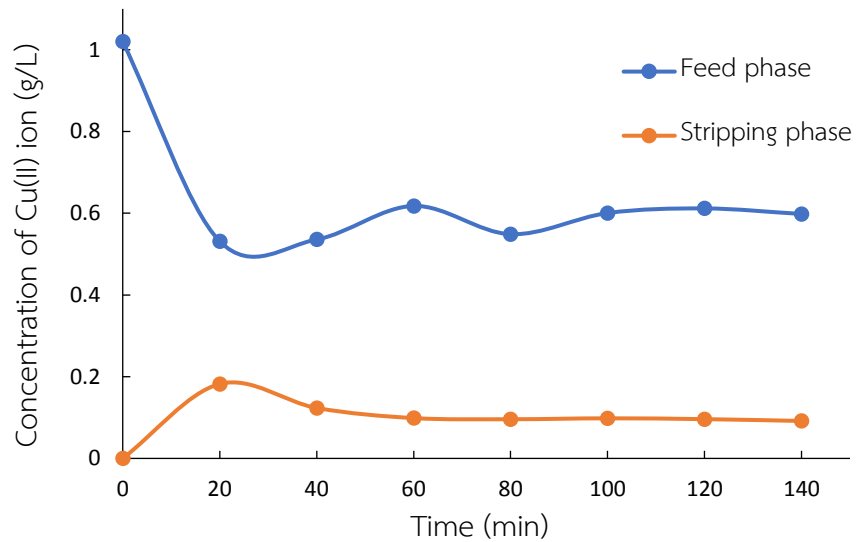


Figure 59 The concentration of Cu(II) ion in the feed phase and stripping phase at any time (membrane thickness = 361.13 μm)

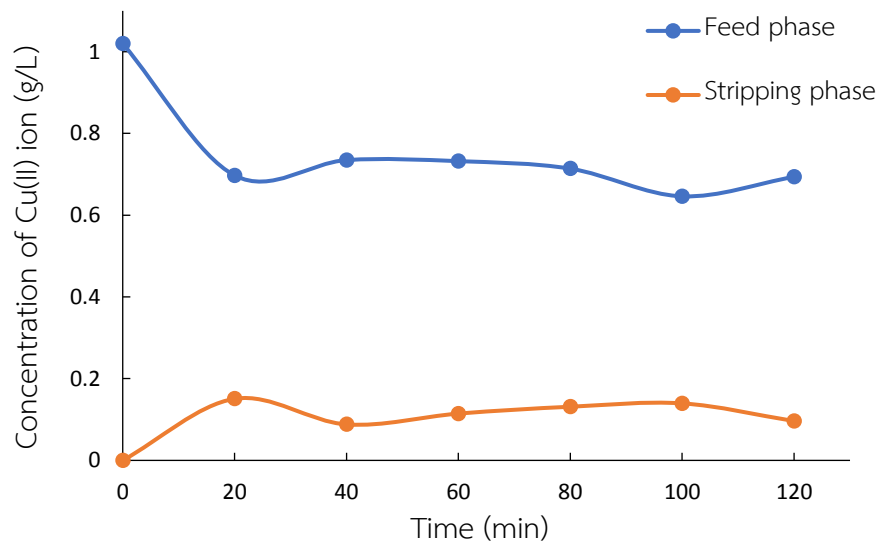


Figure 60 The concentration of Cu(II) ion in the feed phase and stripping phase at any time (membrane thickness = 497.48 μm)

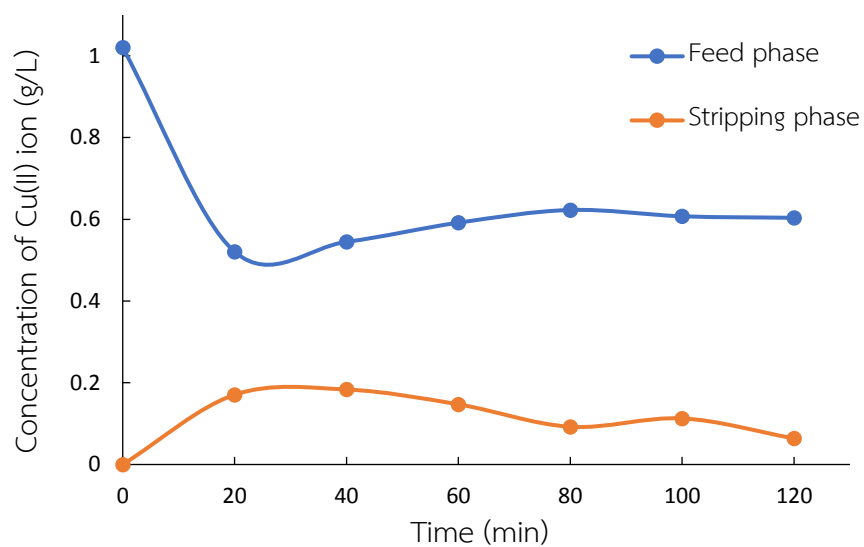


Figure 61 The concentration of Cu(II) ion in the feed phase and stripping phase at any time (membrane thickness = 829.87 μm)



REFERENCES

1. Ma, H., O. Kökkılıç, and K.E. Waters, *The use of the emulsion liquid membrane technique to remove copper ions from aqueous systems using statistical experimental design*. Minerals Engineering, 2017. **107**: p. 88-99.
2. Zhang, W., C. Cui, and Z. Hao, *Transport Study of Cu(II) Through Hollow Fiber Supported Liquid Membrane*. Chinese Journal of Chemical Engineering, 2010. **18**(1): p. 48-54.
3. Raja Sulaiman, R.N. and N. Othman, *Synergetic facilitated transport of nickel via supported liquid membrane process by a mixture of Di (2-ethylhexyl) phosphoric acid and n-octanol: Kinetic permeation study and approach for a green process*. Chemical Engineering and Processing - Process Intensification, 2018. **134**: p. 9-19.
4. Jean, E., et al., *Heavy metal ions extraction using new supported liquid membranes containing ionic liquid as carrier*. Separation and Purification Technology, 2018. **201**: p. 1-9.
5. Zhang, W., C. Cui, and Y. Yang, *Mass Transfer of Copper(II) in Hollow Fiber Renewal Liquid Membrane with Different Carriers*. Chinese Journal of Chemical Engineering, 2010. **18**(2): p. 346-350.
6. Parhi, P.K., *Supported Liquid Membrane Principle and Its Practices: A Short Review*. Journal of Chemistry, 2013. **2013**: p. 11.
7. Zheng, H., et al., *Recovery of Copper Ions from Wastewater by Hollow Fiber Supported Emulsion Liquid Membrane*. Chinese Journal of Chemical Engineering, 2013. **21**(8): p. 827-834.
8. DŻygiel, P. and P.P. Wiczorek, *Chapter 3 - Supported Liquid Membranes and Their Modifications: Definition, Classification, Theory, Stability, Application and Perspectives*, in *Liquid Membranes*, V.S. Kislik, Editor. 2010, Elsevier: Amsterdam. p. 73-140.
9. Kang, G.-d. and Y.-m. Cao, *Application and modification of poly(vinylidene fluoride) (PVDF) membranes – A review*. Journal of Membrane Science, 2014.

- 463**: p. 145-165.
10. Ji, J., et al., *Poly(vinylidene fluoride) (PVDF) membranes for fluid separation*. *Reactive and Functional Polymers*, 2015. **86**: p. 134-153.
 11. Motamedi, A.S., et al., c. *Progress in Biomaterials*, 2017. **6**(3): p. 113-123.
 12. Shen, J., et al., *Liquid Membranes*, in *Nanostructured Polymer Membranes*. 2016. p. 329-390.
 13. Sastre, A.M., et al., *Improved Techniques in Liquid Membrane Separations: An Overview*. *Separation and Purification Methods*, 1998. **27**(2): p. 213-298.
 14. Ahmad, A.L., et al., *Emulsion liquid membrane for heavy metal removal: An overview on emulsion stabilization and destabilization*. *Chemical Engineering Journal*, 2011. **171**(3): p. 870-882.
 15. Gabelman, A. and S.-T. Hwang, *Hollow fiber membrane contactors*. *Journal of Membrane Science*, 1999. **159**(1): p. 61-106.
 16. Boyadzhiev, L. and Z. Lazarova, *Chapter 7 Liquid membranes (liquid pertraction)*, in *Membrane Science and Technology*, R.D. Noble and S.A. Stern, Editors. 1995, Elsevier. p. 283-352.
 17. Lee, J.-c., et al., *Separation of Copper and Zinc Ions by Hollow Fiber Supported Liquid Membrane Containing LIX84 and PC88A*. 2004. **45**: p. 1915-1919.
 18. Kocherginsky, N.M. and Q. Yang, *Big Carrousel mechanism of copper removal from ammoniacal wastewater through supported liquid membrane*. *Separation and Purification Technology*, 2007. **54**(1): p. 104-116.
 19. Mahdavi, H.R., et al., *Pertraction of l-lysine by supported liquid membrane using D2EHPA/M2EHPA*. *Chemical Engineering and Processing: Process Intensification*, 2016. **106**: p. 50-58.
 20. Juang, R.-S. and K.-H. Lin, *Ultrasound-assisted production of W/O emulsions in liquid surfactant membrane processes*. *Colloids and Surfaces A: Physicochemical and Engineering Aspects*, 2004. **238**(1): p. 43-49.
 21. Chiha, M., et al., *Study on ultrasonically assisted emulsification and recovery of copper(II) from wastewater using an emulsion liquid membrane process*. *Ultrasonics Sonochemistry*, 2010. **17**(2): p. 318-325.
 22. Kavitha, N. and K. Palanivelu, *Recovery of copper(II) through polymer inclusion*

- membrane with di (2-ethylhexyl) phosphoric acid as carrier from e-waste. *Journal of Membrane Science*, 2012. **415-416**: p. 663-669.
23. Parhi, P.K. and K. Sarangi, *Separation of copper, zinc, cobalt and nickel ions by supported liquid membrane technique using LIX 84I, TOPS-99 and Cyanex 272*. *Separation and Purification Technology*, 2008. **59**(2): p. 169-174.
 24. Ren, et al., *Extraction Equilibria of Copper(II) with D2EHPA in Kerosene from Aqueous Solutions in Acetate Buffer Media*. *Journal of Chemical & Engineering Data*, 2007. **52**(2): p. 438-441.
 25. W. Reed, B., M.J. Semmens, and E. Cussler, "Membrane contactors," in *Membrane Separations Technology—Principles and applications*,. 1995. **2**: p. 467-498.
 26. Kemperman, A., et al., *Stability of Supported Liquid Membranes: State of the Art*. Vol. 31. 1996. 2733-2762.
 27. Kebiche-Senhadji, O., et al., *Facilitated Cd(II) transport across CTA polymer inclusion membrane using anion (Aliquat 336) and cation (D2EHPA) metal carriers*. *Journal of Membrane Science*, 2008. **310**(1): p. 438-445.
 28. Alguacil, F.J. and M. Alonso, *Description of transport mechanism during the elimination of copper(II) from wastewaters using supported liquid membranes and Acorga M5640 as carrier*. *Environ Sci Technol*, 2005. **39**(7): p. 2389-93.
 29. Alguacil, F.J., M. Alonso, and A.M. Sastre, *Modelling of mass transfer in facilitated supported liquid membrane transport of copper(II) using MOC-55 TD in Iberfluid*. *Journal of Membrane Science*, 2001. **184**(1): p. 117-122.
 30. O'Hara, P.A. and M.P. Bohrer, *Supported liquid membranes for copper transport*. *Journal of Membrane Science*, 1989. **44**(2): p. 273-287.
 31. de Haan, A.B., P.V. Bartels, and J. de Graauw, *Extraction of metal ions from waste water. Modelling of the mass transfer in a supported liquid-membrane process*. *Journal of Membrane Science*, 1989. **45**(3): p. 281-297.
 32. Ren, Z., et al., *New liquid membrane technology for simultaneous extraction and stripping of copper(II) from wastewater*. *Chemical Engineering Science*, 2007. **62**(22): p. 6090-6101.
 33. Sarangi, K. and R.P. Das, *Separation of copper and zinc by supported liquid*

- membrane using TOPS-99 as mobile carrier. Hydrometallurgy, 2004. 71(3): p. 335-342.*
34. Liu, F., et al., *Progress in the production and modification of PVDF membranes. Journal of Membrane Science, 2011. 375(1): p. 1-27.*
35. Technology, S.D., *PVDF (Polyvinylidene fluoride). 2015, Yishida Industrial.*
36. Tichý J., et al., *Fundamentals of Pizelectric Sensorics. Berlin: Berlin Heidelberg, Springer-Verlag, 2010.*
37. Gopal, R., et al., *Electrospun nanofibrous filtration membrane. Journal of Membrane Science, 2006. 281(1): p. 581-586.*
38. Tanimu, A., S. Jaenicke, and K. Alhooshani, *Heterogeneous catalysis in continuous flow microreactors: A review of methods and applications. Chemical Engineering Journal, 2017. 327: p. 792-821.*



VITA

NAME Nattakarn Chucherf

DATE OF BIRTH 04 Nov 1994

PLACE OF BIRTH Songkhal, Thailand

INSTITUTIONS ATTENDED Chemical Engineering, Mahidol in Bachelor of Engineering

HOME ADDRESS 76 soi 2 Santiraj Road Tambon Hatyai, Amphoe Hatyai, Songkhal, Thailand, 90110

PUBLICATION Nattakarn Chucherf, Varong Pavarajarn, "Reactive Extraction of Metal Ion and Simultaneous Stripping Using Nanofibers-Supported Liquid Membrane in a Microchannel". Proceedings of The Pure and Applied Chemistry International Conference 2018 (PACCON 2019), Thailand.